



OPEN

Thermal power plant proximity alters Olive composition and induces cytotoxicity in human cells

Esra Gürbüz^{1,2}, Emre Aksoy³, Aytül Sandallı⁴, Funda Bilgili Tetikoğlu^{1,2}, Enes Şeker¹, Naciye Nisa Kiran¹, Sinan Tetikoğlu^{1,2}, Hacer Muratoğlu¹, Muhammed Fatih Kaya³, Emine Akyüz Turumtay^{5,6,7} & Selcen Çelik Uzuner¹✉

Thermal power plants (TPPs) are essential for meeting increasing energy demands, but they also pose significant environmental and health risks. The Yatağan TPP in Türkiye is located near agricultural and residential areas, raising concerns about its impact on olive trees (*Olea europaea* L.), a key component of the Mediterranean diet. However, the effects of TPP proximity on olive composition and their potential cytotoxicity in human cells remain unknown. This study investigated the biochemical, elemental, and biological responses of olives grown at varying distances (close, middle, and distant) from the Yatağan TPP. Our findings showed that (1) phenolic and flavonoid profiles, as well as fundamental biochemical properties, varied significantly across locations, (2) essential nutrients (Ca, Mg, Fe, Mn) were reduced considerably in olives near the TPP, while toxic metals (As, Cd, Cr, Ni, Pb) accumulated at concerning levels, (3) extracts from olives grown closest to the TPP exhibited cytotoxic effects on normal human cells derived from the breast, retina, vein, and bronchus, and (4) all olive extracts displayed the highest antimicrobial activity against *Staphylococcus aureus*, regardless of their distance from the TPP. These results indicate that industrial emissions disrupt mineral nutrient uptake and elevate toxic metal accumulation in olive trees, potentially affecting food safety and human health. This study highlights the need for continuous environmental monitoring and regulatory measures to mitigate heavy metal contamination and ensure the sustainability of olive cultivation in regions surrounding TPPs.

Keywords Heavy metal accumulation, Elemental concentrations, Food safety, Environmental pollution, Human cell lines, MTT assay, Phenolic compounds

The olive tree (*Olea europaea* L.) is central to the Mediterranean diet, with its fruits and olive oil being essential in gastronomy. Olive leaves have also been widely used in traditional medicine due to their rich bioactive compounds, particularly flavonoids and phenolic compounds, which exhibit anti-oxidant, anti-inflammatory, anti-microbial, and cardioprotective effects¹. Flavonoids like luteolin and luteolin-7-O-glucoside promote erythroid differentiation in stem cells, aiding blood disorder treatment, and facilitating tumor cell apoptosis, highlighting their role in cancer prevention². Among phenolic compounds, oleuropein supports cardiovascular health, while oleocanthal, found in extra virgin olive oil, has anti-inflammatory properties comparable to ibuprofen, making it a promising agent for inflammatory diseases³. Protocatechuic acid and gallic acid neutralize free radicals, offering protection against oxidative stress-related conditions. Ferulic acid further supports cardiovascular health through its antioxidant effects. These bioactive metabolites emphasize the therapeutic potential of olive leaves, strengthening their importance in disease prevention and traditional medicine.

Heavy metal stress severely disrupts plant growth by inducing oxidative stress through the overproduction of reactive oxygen species (ROS), which damage cellular structures, inhibit photosynthesis, and impair essential metabolic processes. To counteract this toxicity, olive trees activate defense mechanisms that involve the increased production of secondary metabolites, particularly flavonoids and phenolic compounds^{4,5}. These bioactive

¹Department of Molecular Biology and Genetics, Faculty of Science, Karadeniz Technical University, Trabzon 61080, Türkiye. ²Graduate School of Natural and Applied Science, Karadeniz Technical University, Trabzon 61080, Türkiye.

³Department of Biological Sciences, Faculty of Arts and Science, Middle East Technical University, 06100 Ankara, Türkiye. ⁴Department of Biology, Faculty of Science, Karadeniz Technical University, Trabzon 61080, Türkiye.

⁵Department of Chemistry, Faculty of Science and Art, Recep Tayyip Erdogan University, Rize 53100, Türkiye.

⁶Joint Bioenergy Institute (JBEI), 5885 Hollis Street, Emeryville, CA 94608, U.S.. ⁷Biological Systems & Engineering Division, Lawrence Berkeley National Laboratory, Berkeley, CA 94720, U.S.. ✉email: selcen.celik@ktu.edu.tr

molecules act as potent antioxidants, scavenging ROS, stabilizing cellular membranes, and chelating heavy metals to reduce their bioavailability. Exposure to heavy metals triggers the upregulation of key enzymes such as phenylalanine ammonia-lyase (PAL) and tyrosine ammonia-lyase (TAL), which are central to the biosynthesis of phenolic compounds⁶. This enzymatic response results in a significant accumulation of protective metabolites, strengthening the plant's ability to tolerate metal-induced stress. By enhancing their antioxidant capacity and detoxification pathways, olive trees improve their resilience against metal toxicity, ensuring their survival in contaminated environments. Moreover, in arid regions with low rainfall, farmers use marginal water sources, such as treated wastewater, for irrigation, increasing the risk of soil contamination with heavy metals like lead (Pb), cadmium (Cd), manganese (Mn), and copper (Cu)⁷. Olive trees, recognized as bioaccumulators of Cu, Pb, and zinc (Zn)⁸ absorb these metals, potentially introducing them into the food chain. Thus, reducing heavy metal contamination in water and soil is crucial for food safety and environmental sustainability.

Thermal power plants (TPP) emit fly ash that contains heavy metals such as arsenic (As), mercury (Hg), Pb, Cd, chromium (Cr), nickel (Ni), and zinc (Zn), which accumulate in the soil. Studies conducted on soil samples from TPPs in various parts of the world have shown significant to extremely high levels of heavy metal contamination^{9–14}. The leaching of these metals into groundwater further extends pollution to larger areas¹⁵ impacting both terrestrial and aquatic ecosystems. For instance, exposure to heavy metals from TPP emissions induces numerous physiological and behavioral effects in organisms, including aquatic insects, amphibians, fish, and mammals¹⁶. In Türkiye, the Yatağan TPP serves as a major point source of heavy metal emissions, with Pb concentrations in lichens and mosses reaching 70.95 µg/g, far exceeding the background level of 22.05 µg/g¹⁷. A recent study in the same area confirmed these findings, suggesting that heavy metal emissions from TPPs significantly alter terrestrial ecosystems¹⁸. Due to bioaccumulation and biomagnification, these pollutants pose severe risks to human health, contributing to increased rates of cancer, as well as heart, liver, and lung diseases¹⁹.

Like other organisms, plants absorb heavy metals, which can lead to toxicity and physiological stress, ultimately reducing their quality and yield²⁰. A study on scarlet firethorn (*Pyracantha coccinea* Roem.) from the same region found a significant accumulation of Pb, Cu, Cd, Ni, and Fe in the leaves²¹. Similarly, a long-term study on Turkish pine (*Pinus brutia*) trees around the Yatağan TPP revealed that annual ring widths significantly decreased in trees located closer to the power plant, based on a 21-year observation period²². The reduction in annual ring width is a clear physiological indicator of stress in trees, reflecting inhibited cambial activity and reduced radial growth, typically caused by chronic exposure to environmental stressors such as heavy metals or air pollution^{23,24}. Comparable results were observed in black pine (*Pinus nigra* Arnold.) near another TPP in Türkiye, where ring sizes significantly declined 25 years after the plant's establishment, particularly in trees closer to the facility²⁵. Further evidence of heavy metal accumulation comes from olive trees in the Yatağan region. A study analyzing olive leaves collected 4 km and 40 km from the TPP showed that Cr, Ni, and Pb accumulated at toxic levels in the closer location, despite soil concentrations of these metals, except for Ni, remaining within normal ranges²⁶. Another study in the same region confirmed that olive trees accumulated significantly higher levels of Pb and Cd²⁷.

While the environmental and ecological risks of TPP emissions are well-documented, their potential impact on human health through olive consumption remains unexplored. Given the central role of olives in the Mediterranean diet, understanding the effects of heavy metal accumulation in olive trees near TPPs is critical. This study aims to bridge this knowledge gap by examining the physiological responses of olive trees (*O. europaea* L.) to heavy metal exposure and assessing the accumulation of these metals in their leaves and fruits. We analyzed phenolic compound levels in olives grown at varying distances from the Yatağan TPP (close, middle, and distant locations) to determine whether pollution alters their bioactive properties. Furthermore, to assess potential health risks, we investigated the cytotoxic effects of olive leaf and fruit extracts on four types of normal human cells (breast, retina, vein, and bronchus). Additionally, we evaluated the antimicrobial properties of these extracts. By integrating plant physiology, food safety, and biomedical perspectives, this *in vitro* study provides important insights into the effects of industrial pollution on olive trees and highlights potential risks for human health within the food chain, warranting further *in vivo* investigation.

Materials and methods

Plant sample collection, morphophysiological properties, and Preparation of plant extracts

Olive fruits and leaves were collected from orchards of Memecik cultivar located in Şahinler Village, Yatağan Center, and Destin Village in the Yatağan district of Muğla province, Türkiye, on October 15, 2022 (Figure S1A). The sampling locations were situated at varying distances from the TPP: 0.8 km, 5.1 km, and 13 km away from the plant, respectively (Figures S1B, S1C, and S1D). A minimum of fifty fruits and leaves were collected from different parts of each of four olive trees of the same age and subsequently pooled. The abbreviations for the locations used throughout the study are as follows: D; Deştin (the furthest location), M (the middle location; Yatağan Center), -T (thermal location; Şahinler Village) and F (fruit), L (leaves). The average annual and October-specific temperatures and precipitation in Yatağan between the 2004–2024 period and 2022 are provided in Table S1. These data suggest that 2022 conditions were generally similar to the multi-year averages in Yatağan.

Olive fruits and leaves were dried at ambient room temperature for 20 days, protected from direct sunlight. Then, fruit and leaf dry weights were determined by a precision analytical balance. Afterward, the dried samples were first coarsely ground using a ceramic grinder, then finely powdered with a ceramic mortar and pestle. To prevent heat buildup from friction, the grinding process was paused every 5 min. For extraction, 40 g of each powdered sample was mixed with 150 mL of 100% methanol in an Erlenmeyer flask, which was then covered with aluminum foil. The samples were incubated in a shaker at 350 rpm for 6 h at room temperature. After incubation, the extracts were filtered into evaporation flasks using Whatman filter paper. The remaining solid

material was subjected to a second extraction with the same amount of solvent under the same conditions for another 6 h. The collected filtrates were then concentrated by evaporating the solvent using a Rotary Evaporator at 40 °C until a dense-liquid extract was obtained. Subsequently, the liquid extracts were freeze-dried using a lyophilizer, and the lyophilized samples were stored at 4 °C. For further use, the extracts were dissolved in 100% DMSO (mg/mL), aliquoted into 60–80 µL portions, and stored at –20 °C.

HPLC-DAD and HPLC-MS conditions for separation of phenolic compounds

Dried samples were dissolved in methanol (40 gram sample in 150 mL methanol) on a shaker for 6 h at room temperature, and then diluted with an equal volume of water (1:1 methanol: water) to achieve suitable concentrations for HPLC-DAD analysis (DL: 10 mg·mL⁻¹, DM: 50 mg·mL⁻¹, ML: 20 mg·mL⁻¹, MM: 100 mg·mL⁻¹, TL: 10 mg·mL⁻¹, and TF: 57 mg·mL⁻¹). Final extract-to-solvent ratios ranged from 1.0 to 10.0% (w/v) depending on the sample: DL (1.0%), DM (5.0%), ML (2.0%), MM (10.0%), TL (1.0%), and TF (5.7%). Extracts were centrifuged at 10,000 rpm for 15 min before HPLC-DAD analysis. The chromatographic analyses were then performed using a Dionex (Thermo Scientific, Germering, Germany) Ultimate 3000 high-performance liquid chromatography (HPLC) system equipped with an Ultimate 3000 diode array detector (DAD). A Thermo acclaim C30 column (150 mm. 3 mm id. 3 µm pd) was used with a Macherey Nagel (3 mm id) guard column. Gradient elution was used with mobile phases; A: 2% acetic acid in water and B: 70% acetonitrile-30% water. The flow rate was 0.37 mL/min, and the injection volume was 10 µL. Column temperature was set at 25 °C. The following 25 phenolic standards were used to calibrate and validate the HPLC-DAD analysis method: Gallic acid, protocatechuic acid, p-hydroxy benzoic acid (p-OH benzoic acid), chlorogenic acid, vanillic acid, caffeic acid, syringic acid, vanillin, epicatechin, p-coumaric acid, ferulic acid, rutin, luteolin-7-glycoside, naringin, hesperidin, apigenin-7-glycoside, rosmarinic acid, fisetin, eriodictyol, luteolin, quercetin, naringenin, hesperetin, apigenin, and kaempferol. These standards were diluted from their stock solutions into nine different concentrations at 0.625; 1.25; 5.0; 10.0; and 20.0 µg·mL⁻¹ in a 1:1 methanol-water solution for the external calibration. Repeatability of the retention time (RT) and peak areas was measured as coefficient of variation (CV) which was under 0.61 for retention times and under 3.60 for areas of the peaks. The limit of detection (LOD) and quantification (LOQ) values of all standards were under 0.18 and 0.52 µg/mL (Table S2). Chromatograms were processed at 254, 280, 315, and 370 nm with DAD, which operated at 200–400 nm. The identification of the peaks was carried out by comparing the RT and UV spectra with those of standard phenolic compounds. Some peaks had the same or similar UV spectra as some standards, but with different retention times (RTs). They were defined as derivatives of standards with similar UV spectra and quantified as the equivalent of those standards. The peaks with different spectra from all standard compounds were characterized using the results of the reports studied to identify the compound of this plant species. For instance, the spectrum of oleuropein aglycone, nüzenide 11-methyl oleoside, and oleocanthal was reported in olive extracts^{28,29}. Peaks with spectra similar to those of these three compounds were characterized as their derivatives and measured as the equivalent of protocatechuic acid using peak areas at 254 nm. The calibration and validation parameters of the HPLC-DAD method are presented in Table S2. We collected samples at once so that HPLC was performed once for each extract; instead, method validation was used with repeatability values of the standard mixes.

Human cell culture, extract treatments, and MTT assay

The healthy cell lines used in this study are commercial. The cells included MCF10A (ATCC, CRL-10317[™]) human mammary gland epithelial cells, ARPE-19 (ATCC, CRL-2302[™]) human eye retinal pigment epithelial cells, HUVEC (ATCC, CRL-1730[™]) primary human umbilical vein endothelial cells, and BEAS-2B (ATCC, CRL-3588[™]) epithelial cells isolated from normal human bronchial epithelium. Except for BEAS-2B cells, which were cultured in DMEM, other cells were cultured in RPMI media, including 10% fetal bovine serum and 1% penicillin-streptomycin. Cells were incubated at 37 °C with 5% CO₂ until they reached full confluence, at which point they were transferred to 96-well plates for further treatment. Confluent cells were treated with fruit and leaf extracts at final concentrations of 500 µg/mL, 100 µg/mL, 20 µg/mL, 4 µg/mL, 0.8 µg/mL, 0.16 µg/mL, and 0.032 µg/mL for either 24–48 h. Untreated control cells (0 µg/mL) were included for comparison. Following the treatment period, the culture media were removed, and 190 µL of fresh media along with 10 µL of 0.25 mg/mL MTT ((3-(4,5-Dimethylthiazol-2-yl)-2,5-Diphenyltetrazolium Bromide) dye were added to each well. Next, the plates were incubated at 37 °C for 2 h. After incubation, MTT-containing media were removed, and 200 µL of DMSO was added to each well to dissolve the purple formazan crystals formed by the reduction of MTT in metabolically active cells. Since formazan is insoluble in aqueous solutions, DMSO ensures complete solubilization, resulting in a uniform colored solution. The plates were then placed in a shaker at 120 g for 1 h at dark to dissolve the formazan crystals. Absorbance measurements were taken at 570 nm using a spectrophotometer^{30,31}. The absorbance of untreated cells was considered 100% viability, and the viability of treated cells was calculated relative to the absorbance of the untreated control group. The most straightforward way to estimate IC₅₀ is by plotting the x-y data and applying linear regression. The IC₅₀ value is then determined from the fitted line by the formula $Y = a * X + b$, $IC_{50} = (0.5 - b)/a$. For statistical analyses, cell percentages were arcsine transformed using the formula = ASIN(SQRT(X/100)) * 180/PI() (X represents a value of cell percentage) to fit data for UNIANOVA statistical analyses.

Elemental analyses

Olive leaf and fruit samples collected from the field were first dried at 65 °C for 2 days, then ground into a fine powder using a grinder. Approximately 100 mg of the ground samples were then transferred into fresh 50 mL Falcon tubes. Then, approximately 100 mg of the samples were placed in fresh 50 mL Falcon tubes. A total of 3 mL of 65% nitric acid (Sigma-Aldrich) and 2.15 mL of 35% hydrogen peroxide (Sigma-Aldrich) were added to each tube. The lids of the Falcon tubes were loosely closed, and the samples were incubated at 80 °C for

approximately 8 h until no visible particles remained. The liquid samples were then filtered, transferred into fresh Falcon tubes, and diluted 10 times to bring the final nitric acid concentration to 2%. The diluted samples were analyzed using Inductively Coupled Plasma Mass Spectrometry (ICP-MS) (Perkin Elmer DRC II). The mineral content was calculated by dividing the absorbance values by the dry weights.

Anti-microbial and antifungal activity of fruit and leaf extracts

Collected and extracted six olive fruit and leaf samples (DL, DF, ML, MF, TL, TF) were assayed for their anti-microbial and antifungal activities. Common six pathogenic bacteria and yeast-like fungi were used for these tests. Pathogenic bacteria selected as gram-negative bacteria are *Escherichia coli* (ATCC 25922), *Yersinia pseudotuberculosis* (ATCC 911), and *Pseudomonas aeruginosa* (ATCC 17853). Other pathogenic bacteria selected as gram-positive bacteria are *Staphylococcus aureus* (ATCC 25923), *Enterococcus faecalis* (ATCC 29212), and *Bacillus subtilis* (ATCC 10876). Another pathogenic microorganism that we studied was yeast-like fungi, *Candida albicans* (ATCC 10231). Minimum inhibitory concentration (MIC) values (µg/mL) of extracts were determined by the microtiter broth dilution method using rapid INT (iodonitrotetrazolium chloride) colorimetric assay based on the Clinical and Laboratory Standards Institute (CLSI) guidelines³². First, the maximum soluble concentrations of the six extracts were determined by dissolving them in DMSO. Stock concentrations were 50 mg/mL for DL, 50 mg/mL for TL, 55 mg/mL for ML, 50 mg/mL for MF, 40 mg/mL for TF and 60 mg/mL for DF. Stock concentrations were diluted 2-fold with Mueller-Hinton broth (MHB) and added to the 96-well plate as 100 µL/well. Then, bacteria were added as 5×10^{-5} CFU (colony-forming units)/mL for each well. Microplates were incubated at 37 °C for 24 h. After that, 40 µL of 0.2 mg/mL INT was added to each well and incubated at 37 °C for 30 min. A representative microplate design is given in Figure S2. The results were evaluated by whether the indicator resulted in a pink color. The pink color indicates bacterial growth. The colorless first dose gives the MIC value. To determine the MIC values, experiments were performed as three independent replicates and at least 2 replicates within the experiment. Ampicillin (50 mg/mL) was used to inhibit bacteria, and kanamycin (50 mg/mL) was used to inhibit yeast-like fungi as an experimental positive control. An experiment was also designed to calculate MIC values for these antibiotics. An experiment was designed to determine the MIC value of DMSO on microorganisms as a negative control (Figure S3). The MIC values of all extracts were determined according to the non-toxic DMSO dose. Toxic doses of DMSO in dissolved extracts were neglected in experiments.

Statistical analyses

Cell viabilities (%) (arcsine transformed) were compared using the UNIANOVA test of the SPSS program (Version 13.0). Plant morphophysiological measurements were compared by one-way ANOVA followed by Tukey's HSD test whereas element concentration measurements were compared by Student's t-test. *p* values less than 0.05 were considered significant in statistical analyses. Significance levels used for cytotoxicity analyses were as follows, * *p* < 0.05, ** *p* < 0.01, *** *p* < 0.001, and **** *p* < 0.0001, and asterisks were indicated on the bar graphs.

Results

Effects of TPP proximity on the morphophysiological properties of Olive leaves and fruits

To assess the impact of proximity to the TPP on olive tree growth, we compared the size and dry weight of leaves and fruits collected from trees at varying distances. Samples from Şahinler, the closest site to the TPP, had notably smaller leaves and fruits, whereas the largest fruits were observed in those collected from Deştin, the farthest site (Fig. S1E). The dry weights of both leaves and fruits were significantly higher in Deştin compared to Şahinler, while Yatağan Center showed intermediate values that were not always statistically distinct from either group (Table S3). Leaf dry weight in Deştin was approximately 25% higher, and fruit dry weight about 17% higher than in Şahinler. These differences in size and biomass probably suggest that the TPP's proximity negatively affected plant morphology and physiology, likely due to heavy metal-induced stress.

Effects of TPP proximity on mineral and heavy metal composition of Olive leaves and fruits

To further investigate the potential effects of heavy metal-induced stress on olive trees near the TPP, we analyzed the mineral and heavy metal composition of leaves and fruits from Şahinler and Deştin, the locations showing the most pronounced differences in biomass (Table S3). In general, leaves and fruits from Deştin accumulated significantly higher concentrations of several elements compared to Şahinler (Table 1). For example, Ca levels in leaves from Deştin were 13,832.93 mg/kg versus 1,708.34 mg/kg in Şahinler, an approximate 87.7% decrease in Şahinler. In fruits, Ca dropped even more dramatically, with a 91.7% lower concentration in Şahinler compared to Deştin. Mg concentration in the leaves collected from Şahinler was 596.51 mg/kg compared to 1,241.92 mg/kg in Deştin, representing a 52.0% reduction, while fruits in Şahinler were 62.4% lower than those in Deştin. Na concentrations were 36.5% lower in Şahinler leaves (34.55 mg/kg) compared to Deştin (54.42 mg/kg), and in fruits, Na was 41.4% lower in Şahinler than in Deştin. S in leaves from Şahinler was 16.8% lower than in Deştin, with fruit S levels showing a 39.7% decrease. Al was also noticeably reduced in Şahinler, with leaves showing an 85.9% lower concentration and fruits a 90.5% decrease relative to Deştin. Fe in leaves was 76.7% lower in Şahinler, though in fruits the concentrations were very similar, differing by only a minor margin. Mn in Şahinler leaves was 70.5% lower than in Deştin, and fruit Mn was 68.3% lower. Regarding Zn, although leaves from Şahinler had a 53.7% lower concentration compared to Deştin, the fruit Zn levels were nearly identical between the two locations (a difference of only about 2.2%). On the contrary, several elements were significantly higher in Şahinler. K levels in Şahinler leaves were 177.5% higher than in Deştin, and in fruits, K was 113.8% higher.

For trace and potentially toxic elements, the differences were even more striking. In Şahinler leaves, Co levels were 223-fold higher than in Deştin, while in fruits, Co levels were 29.5-fold higher. Cu concentrations

| Element | Leaf | | Fruit | |
|----------------|------------------|--------------------|------------------|------------------|
| | Deştin (Distant) | Şahinler (Near) | Deştin (Distant) | Şahinler (Near) |
| Macronutrients | | | | |
| Ca | 13832.93 ± 1.43 | 1708.34 ± 2.94 * | 4176.23 ± 0.41 | 349.45 ± 0.01 * |
| K | 6877.04 ± 0.74 | 19085.36 ± 35.09 * | 1808.52 ± 0.73 | 3867.52 ± 1.92 * |
| Mg | 1241.92 ± 0.25 | 596.51 ± 1.12 * | 382.18 ± 0.15 | 143.77 ± 0.10 * |
| Na | 54.42 ± 0.014 | 34.55 ± 0.028 * | 14.29 ± 0.003 | 8.38 ± 0.004 * |
| P | 1019.00 ± 0.23 | 982.41 ± 1.66 | 240.06 ± 0.048 | 269.32 ± 0.074 * |
| S | 909.14 ± 0.07 | 756.55 ± 1.41 * | 374.95 ± 0.03 | 226.24 ± 0.01 * |
| Micronutrients | | | | |
| Al | 62.17 ± 0.039 | 8.76 ± 0.018 * | 12.12 ± 0.007 | 1.16 ± 0.004 * |
| B | 25.88 ± 0.0003 | 25.23 ± 0.0275 | 6.84 ± 0.0016 | 4.88 ± 0.0001 |
| Co | 0.02 ± 3.18E-5 | 4.47 ± 3.18E-3 * | 0.04 ± 2.47E-5 | 1.18 ± 2.47E-3 * |
| Cu | 8.17 ± 0.012 | 45.76 ± 0.038 * | 1.67 ± 0.004 | 13.34 ± 0.006 * |
| Fe | 77.85 ± 0.049 | 18.11 ± 0.054 * | 16.63 ± 0.001 | 14.75 ± 0.016 |
| Mn | 21.35 ± 0.004 | 6.29 ± 0.011 * | 6.13 ± 0.003 | 1.94 ± 0.005 * |
| Mo | 0.39 ± 0.0004 | 0.88 ± 0.0011 * | 0.08 ± 0.0003 | 0.10 ± 0.0003 |
| Ni | 1.26 ± 7.07E-4 | 26.38 ± 0.046 * | 0.18 ± 6.01E-4 | 2.10 ± 0.024 * |
| Zn | 20.78 ± 0.077 | 9.62 ± 0.021 * | 2.74 ± 8.88E-4 | 2.68 ± 2.8E-4 |
| Toxic elements | | | | |
| As | 0.06 ± 3.88E-5 | 4.89 ± 1.41E-3 * | 0.01 ± 5.30E-5 | 0.27 ± 3.88E-4 * |
| Cd | 0.02 ± 3.53E-5 | 3.71 ± 2.47E-3 * | 0.04 ± 7.07E-5 | 0.83 ± 7.07E-4 * |
| Cr | 0.01 ± 7.07E-6 | 4.38 ± 6.7E-3 * | 0.05 ± 7.07E-5 | 0.87 ± 1.44E-3 * |
| Hg | 38.28 ± 0.019 | 54.04 ± 0.023 * | 7.93 ± 0.010 | 10.23 ± 0.072 |
| Pb | 0.28 ± 3.88E-4 | 16.80 ± 0.018 * | 0.04 ± 3.53E-5 | 0.27 ± 3.18E-4 * |

Table 1. Elemental analysis of Olive leaves and fruits collected from two locations depending on their distance to the power plant. Values are provided in mg/kg DW. Mean ± SEM ($n=3$). * Indicates a significant difference between each location ($p < 0.05$).

in Şahinler leaves were approximately 5.6-fold higher than in Deştin, and in fruits, Cu was about 8-fold higher. Ni also showed a dramatic increase, with Şahinler leaves having roughly 20.9-fold higher Ni levels compared to Deştin, and fruits exhibiting about 11.7-fold higher levels. Toxic elements further highlight the impact of proximity to the power plant. As in Şahinler leaves were 81.5-fold higher than in Deştin, with fruits showing a 27-fold increase. Cd in Şahinler leaves was about 185.5-fold higher than in Deştin, and in fruits, Cd levels were approximately 20.8-fold higher. Cr exhibited the most dramatic difference in leaves, with a 438-fold increase in Şahinler relative to Deştin, while in fruits, Cr was about 17.4-fold higher. Hg in Şahinler leaves was 41.2% higher than in Deştin, and fruit Hg concentrations were about 29% higher. Pb levels in Şahinler leaves were 60-fold higher compared to Deştin, while in fruits, Pb was 6.75-fold higher.

For other nutrients, there was no significant difference in P and B concentrations in the leaves between the two locations. However, fruits from Şahinler had a 12.2% higher P concentration than those from Deştin. Mo levels in leaves were significantly higher in Şahinler (a 125.6% increase) compared to Deştin, while in fruits, the Mo concentrations were quite similar between the two locations (only about a 25% difference).

Essential nutrients are tightly connected, indicating their levels tend to drop together while the toxic elements also show strong interconnections, meaning their levels tend to rise together (Fig. 1). Negative interactions highlight the competition or antagonistic effects between heavy metals and essential nutrients. Taken together, our results suggest that samples from Şahinler, located near the Yatağan Thermal Power Plant, show clear signs of heavy metal contamination, with significantly elevated levels of toxic elements such as As, Cd, Cr, Ni, and Pb. At the same time, essential nutrients such as Ca, Mg, Fe, and Mn are reduced, indicating a disruption in mineral nutrient uptake. These results suggest that industrial pollution is altering plant chemistry, leading to both nutrient imbalances and potential toxicity risks.

Biochemical composition of Olive leaves and fruits collected from different distances from TPP

To explore the impact of TPP proximity on the biochemical composition of olive leaves and fruits, we analyzed their metabolite profiles. Metabolites were extracted using methanol, as described in the experimental section, and their chemical composition was determined via HPLC-DAD analysis. Fruit extracts mostly contained key olive-derived compounds such as oleuropein aglycone, nüzhénide 11-methyl oleoside, and oleocanthal (Fig. 2A, Table S4). Among the samples, the DF extract exhibited the highest diversity of compounds, whereas the TF extract had the lowest. Secondary metabolite accumulation in fruit extracts varied by location, with the highest levels generally observed in samples from Deştin, reinforcing the trend of greater metabolite accumulation at the site farthest from the TPP (Fig. 3A, Table S4). Oleuropein aglycone D7, for instance, was 17.4 times

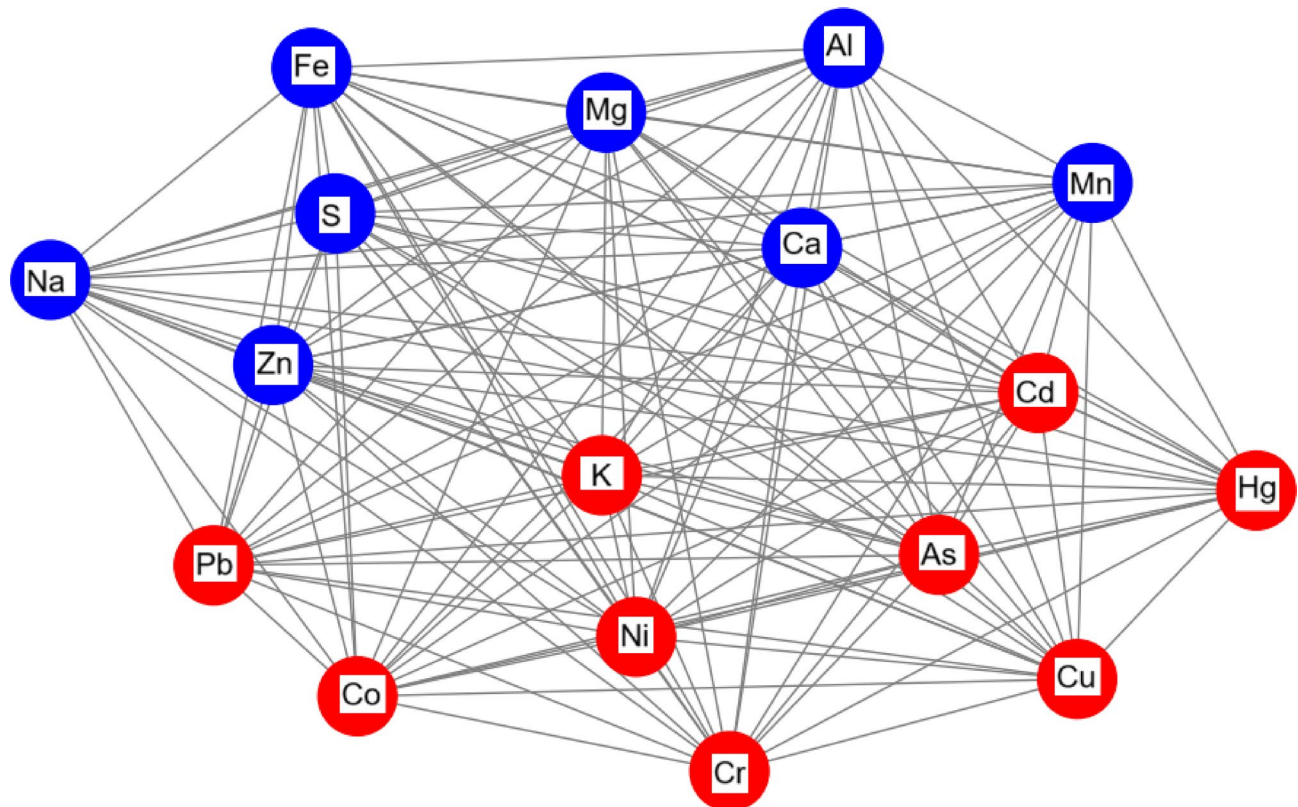


Fig. 1. Correlation network of elemental changes in olive trees. Blue nodes represent downregulated essential nutrients while the red nodes visualize upregulated toxic metals. Edges within each cluster represent positive correlations, and edges between clusters (nutrients vs. toxic elements) represent negative correlations. Generated in Google Colab via Phyton⁹⁰.

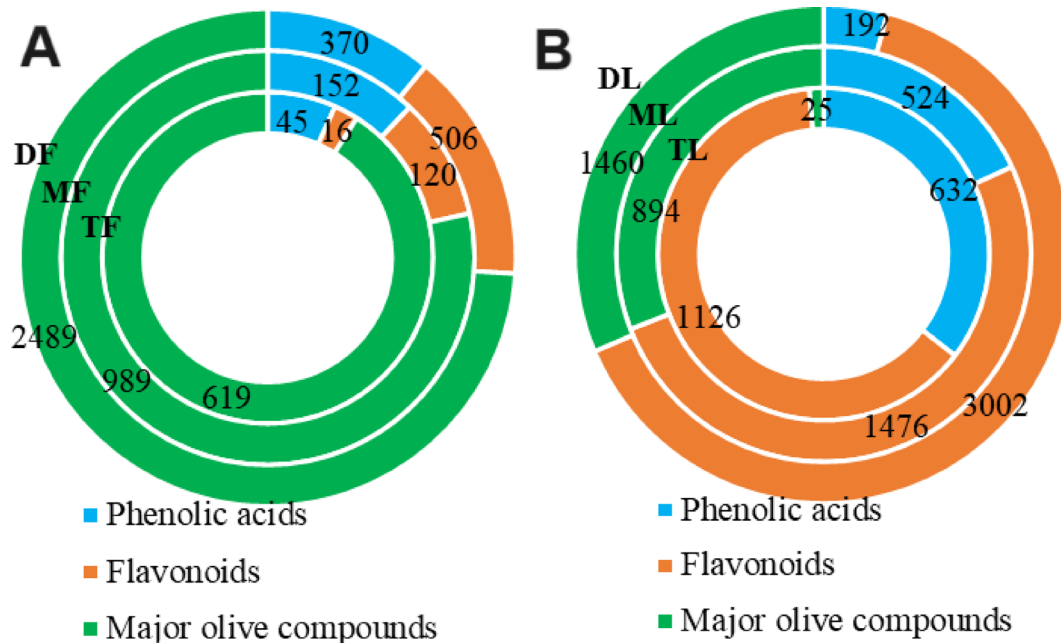


Fig. 2. Chemical composition of (A) the fruit and (B) leaf extracts of the olive samples. Values are presented as mg/100 g extract. *D*: *Destin* (the furthest location), *M* (the middle location; *Yatağan Center*), -*T* (thermal location; *Şahinler Village*) and *F* (fruit), *L* (leaves).

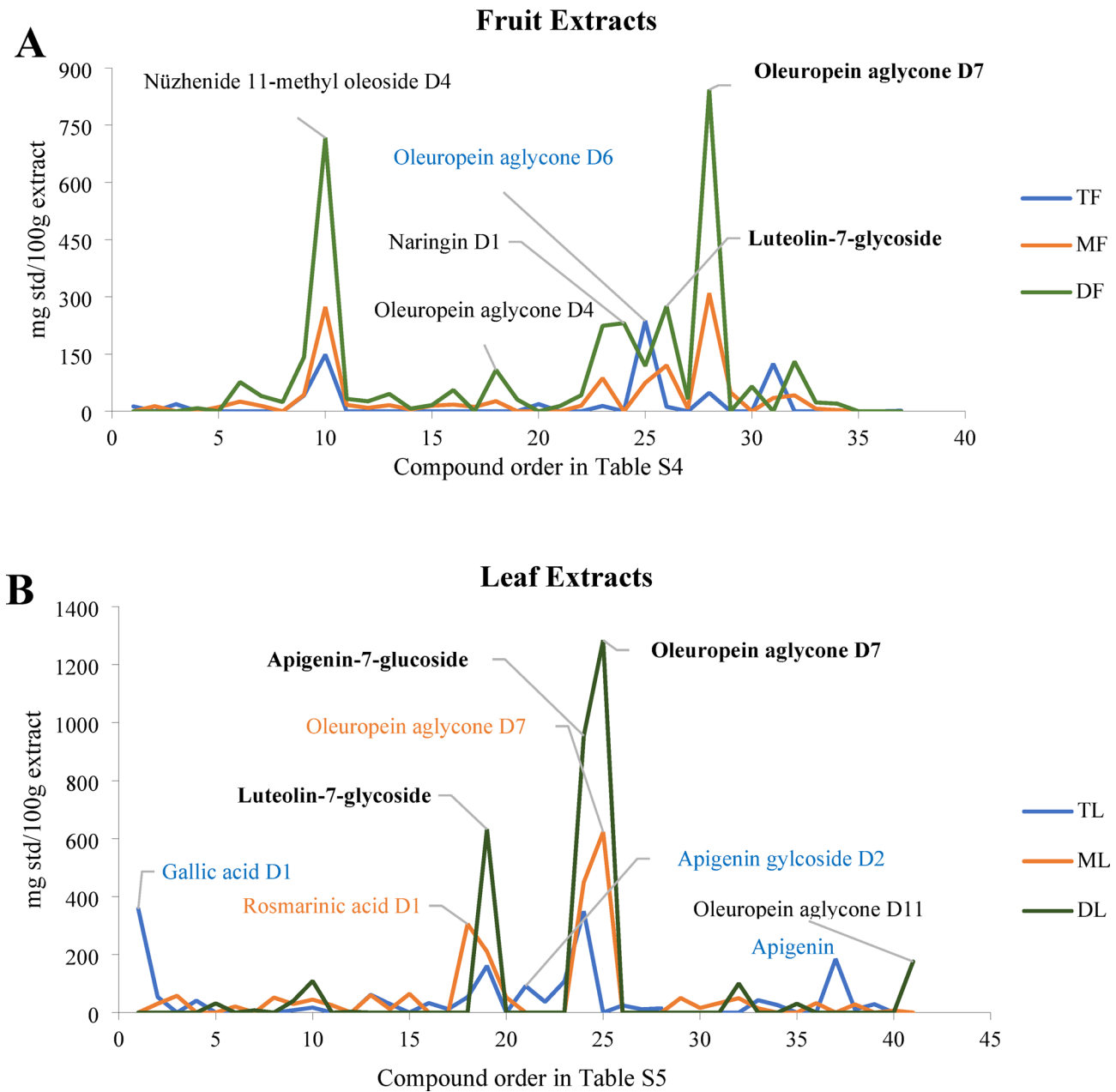


Fig. 3. Changing the chemical composition of (A) fruit and (B) leaf extracts based on their region, plotted according to their order in Table S4 and S5. D; *Deştin* (the furthest location), M (the middle location; *Yatağan* Center), -T (thermal location; *Şahinler* Village) and F (fruit), L (leaves).

more abundant in DF extracts compared to TF extracts, while nüzenide 11-methyl oleoside D3 and D4 were 3.4 and 4.8 times higher, respectively. However, oleuropein aglycone D6 was an exception, accumulating 1.98 times less in DF extracts than in TF extracts (Figs. S4–S6, Table S4). In contrast, MF extracts had the highest concentration of oleuropein aglycone D7, followed by nüzenide 11-methyl oleoside D4 (Fig. S5, Table S4). Interestingly, certain metabolites, such as protocatechuic acid, gallic acid, oleuropein aglycone D5, and apigenin, were exclusively detected in fruit samples from trees near the TPP (TF extracts) but were absent from the other two locations (Table S4).

Oleuropein aglycone D8 was the most abundant compound detected in the leaf extracts, whereas flavonoids were also found at significantly higher levels in leaf extracts compared to fruit extracts (Figs. S7–S9, Table S5). Among the flavonoids, apigenin-7-glucoside was the predominant compound in the leaf extracts, while luteolin-7-glucoside was the most abundant in the fruit extracts (Fig. 2B, Table S5). Notably, both leaf and fruit extracts obtained from *Deştin*, the farthest location from the TPP, contained the highest levels of these bioactive compounds, whereas extracts from *Şahinler*, the closest location to the TPP, had the lowest amounts. The most abundant compounds in the leaf extracts were oleuropein aglycone D7, apigenin-7-glycoside, and luteolin-7-glycoside, with DL extracts exhibiting the highest concentrations (Fig. 3B, Table S5). Similarly, oleuropein

aglycone D7 was found at its highest levels in both DF and DL extracts, particularly in those collected from Deştin. One of the key bioactive secoiridoids in olive leaves, oleuropein, can constitute 6–9% of the dry matter, along with related secoiridoids, flavonoids, and triterpenes¹. Although secondary metabolites such as ferulic acid, luteolin, luteolin glycoside, and apigenin glycoside were also present in the leaves of trees near the TPP (Table S5), their concentrations were lower than those in trees from Deştin, suggesting that environmental factors associated with TPP proximity may influence the accumulation of these bioactive compounds. Taken together, these findings suggest that proximity to the TPP significantly influences the metabolic profiles of olive leaves and fruits, likely due to exposure to heavy metals (Table S6). The lower accumulation of key bioactive compounds in samples from trees closest to the TPP indicates that these stressors may disrupt secondary metabolite biosynthesis, potentially affecting the nutritional and pharmacological properties of olives.

Cytotoxicity profiles of fruit and leaf extracts on human cells

To further investigate the potential implications of these metabolic alterations, we evaluated whether the observed differences in secondary metabolite accumulation influence the biological effects of olive extracts on human cells. Using the previously described treatment conditions, we analyzed the cytotoxic effects of fruit and leaf extracts from different locations on healthy human cell lines after 24 and 48 h of exposure. In ARPE-19 (Fig. 4) and MCF10A (Fig. 5) cells, olive leaf extracts obtained from the closest location to the TPP showed more cytotoxic effects at 100 µg/mL for 48 h than fruit extracts at the conditions ($p < 0.05$). IC50 values of

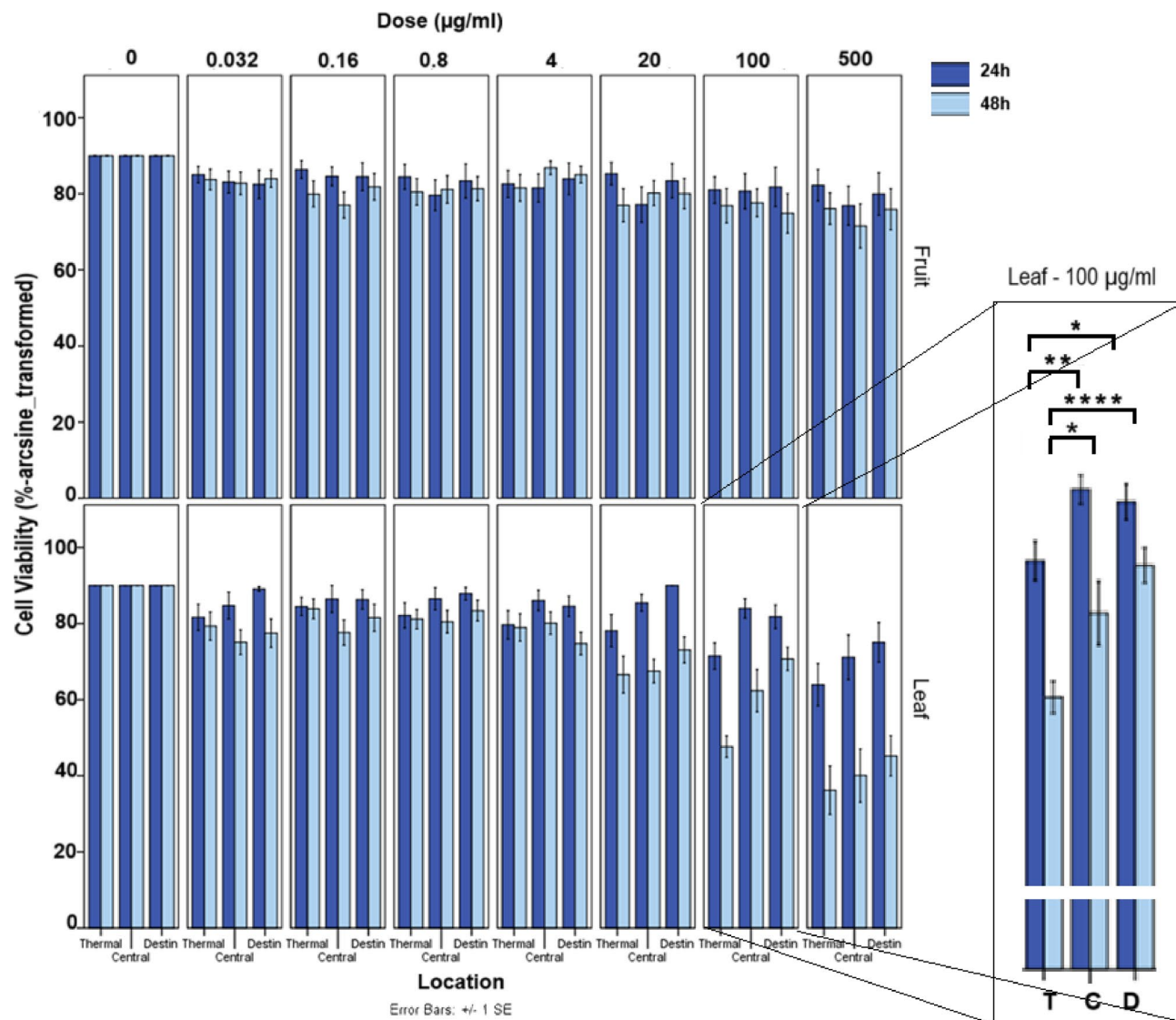


Fig. 4. The cell viability of ARPE-19 human retinal epithelial cells treated with fruit (up panel) and leaf (down panel) extracts at varying concentrations for 24 h and 48 h. Extracts were obtained from olives grown at different distances from the Yatağan TPP, Deştin Village (farthest location), Central (middle location), and Thermal (Şahinler Village - closest location). Values represent mean \pm SEM ($n=3$). * $p < 0.05$, ** $p < 0.01$, *** $p < 0.001$, and **** $p < 0.0001$.

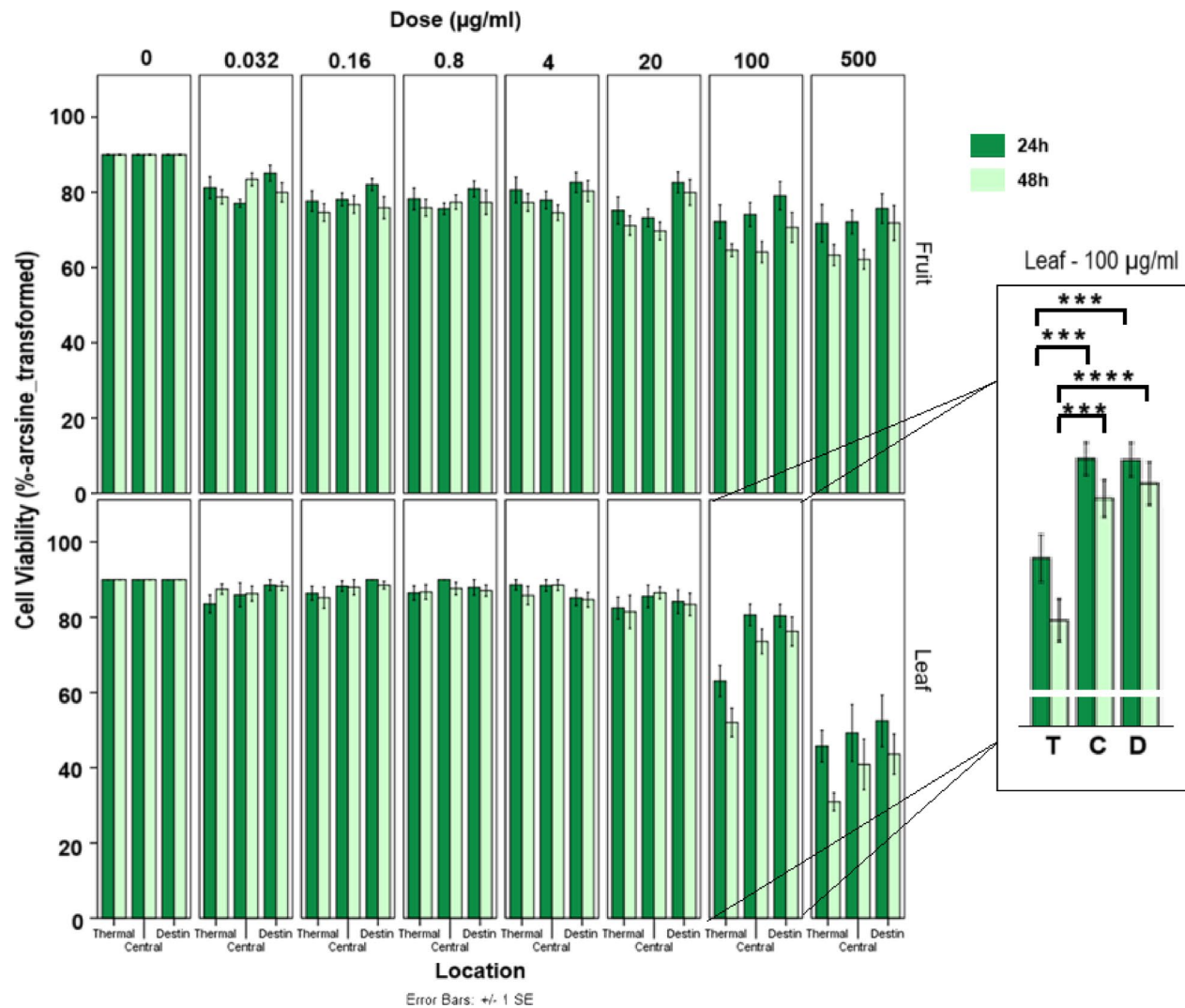


Fig. 5. The cell viability of MCF10A human breast epithelial cells treated with fruit (up panel) and leaf (down panel) extracts at varying concentrations for 24 h and 48 h. Extracts were obtained from olives grown at different distances from the Yatağan TPP, Deştin Village (farthest location), Central (middle location), and Thermal (Şahinler Village - closest location). Values represent mean \pm SEM ($n=3$). * $p < 0.05$, ** $p < 0.01$, *** $p < 0.001$, and **** $p < 0.0001$.

ARPE-19 cells at 48 h were 115,35 $\mu\text{g/mL}$, 126,3 $\mu\text{g/mL}$, and 237,28 $\mu\text{g/mL}$ after treatments with leaf extracts collected from thermal, central, and Destin, respectively (Table 2). MCF10A cells were more resistant, compared to ARPE-19 cells, as IC50 values at 48 h were 287,07 $\mu\text{g/mL}$, 239,1 $\mu\text{g/mL}$, and 486,14 $\mu\text{g/mL}$ after treatments with leaf extracts collected from thermal, central, and Destin, respectively.

The highest cytotoxicity (around 80% cell death) was shown in BEAS-2B cells after 500 $\mu\text{g/mL}$ leaf extract from the thermal location for 48 h, compared to other locations ($p < 0.05$) (Fig. 6), and 100 $\mu\text{g/mL}$ was also significantly cytotoxic if the extract from thermal. IC50 values for thermal, central, and Destin were 127,18 $\mu\text{g/mL}$, 215,07 $\mu\text{g/mL}$, and 248,20 $\mu\text{g/mL}$, respectively (Table 2). Fruit extracts induced similar cytotoxicity at 48 h, and interestingly IC50 dose (555,18 $\mu\text{g/mL}$) was the maximum for thermal fruits, suggesting that thermal leaves were highly cytotoxic for BEAS-2B cells, but thermal fruits were not. There was a similar cytotoxicity profile of HUVEC cells after the treatment with 500 $\mu\text{g/mL}$ leaf extracts of collected forms from both in the center and near the TPP, compared to the further Destin village (Fig. 7). Thermal leaves (500 $\mu\text{g/mL}$) were significantly cytotoxic at 24 h ($p < 0.05$) but not at 48 h. However, thermal fruits at 100 $\mu\text{g/mL}$ and 500 $\mu\text{g/mL}$ were less cytotoxic than samples from other locations (Fig. 7). IC50 values for thermal, central, and Destin after fruit extracts at 48 h were 391,91 $\mu\text{g/mL}$, 270,17 $\mu\text{g/mL}$, and 273,88 $\mu\text{g/mL}$, respectively (Table 2.).

Cell viability comparisons between the cells treated with 100 $\mu\text{g/mL}$ or 500 $\mu\text{g/mL}$ leaf or fruit extracts (48 h) collected from the thermal region are summarized in Table S7. The cytotoxicity results suggest that the leaf extract is more cytotoxic in ARPE-19 and MCF10A cells, and the death rate is similar in all locations after the highest dose (500 $\mu\text{g/mL}$) of leaf extracts. In contrast, 100 $\mu\text{g/mL}$ of leaf extracts from Şahinler, the location closest to the TPP, resulted in cytotoxicity of the cells compared to other locations. Unlike ARPE-19 and MCF10A2, fruit

| Cell | Incubation | 24 hours | | 48 hours | | | |
|---------|------------|----------|---------|----------|---------|---------|--------|
| | | Location | | | | | |
| | Extract | Thermal | Central | Destin | Thermal | Central | Destin |
| ARPE-19 | Fruit | N.D | N.D | N.D | N.D | N.D | N.D |
| | Leaf | N.D | N.D | N.D | 115,35 | 126,30 | 237,28 |
| MCF10A | Fruit | N.D | N.D | N.D | N.D | N.D | N.D |
| | Leaf | N.D | N.D | N.D | 287,07 | 239,10 | 486,14 |
| BEAS-2B | Fruit | 555,18 | 311,85 | 370,17 | 179,11 | 171,68 | 176,10 |
| | Leaf | 281,47 | N.D | N.D | 127,18 | 215,07 | 248,20 |
| HUVEC | Fruit | N.D | 216,11 | 207,80 | 391,91 | 270,17 | 273,88 |
| | Leaf | 406,40 | N.D | N.D | 353,82 | 292,87 | N.D |

Table 2. Average IC50 doses (μg/ml) at 24h and 48h for each cell after extracts collected from different locations N.D. not detectable.

extracts showed more cytotoxic activity in BEAS-2B and HUVEC cells. Table S8 summarizes the comparison of cell viability after treatment with 100 μg/mL or 500 μg/mL leaf or fruit extracts for 48 h, specifically using samples collected from the closest location to the TPP. This selection was made to assess whether exposure to environmental stressors associated with TPP proximity, such as heavy metal accumulation and reduced secondary metabolite content, affects the cytotoxic potential of olive extracts. The cytotoxicity of BEAS-2B cells appears to be more sensitive to the leaf extracts at 100 μg/mL compared to other cells. All cells responded to the highest concentrations (500 μg/mL) of leaf extracts similarly, as no significant differences between the cells were observed. However, after treatment with the highest concentration (500 μg/mL) of fruit extracts for 48 h, statistically significant differences in cell viability were detected. These findings suggest that the increased cytotoxicity of olive extracts from trees closest to the TPP may be attributed to the combined effects of reduced bioactive metabolite accumulation and potential heavy metal contamination. The lower concentrations of key secondary metabolites, such as oleuropein aglycones and flavonoids, in samples from Şahinler could diminish their protective antioxidant properties, while elevated heavy metal exposure may enhance their cytotoxic effects. This interplay highlights the impact of environmental pollution on the biochemical and biological properties of olive-derived products, with potential implications for their nutritional and pharmacological value.

Antimicrobial and antifungal activities of fruit and leaf extracts against pathogenic bacteria and fungi

To evaluate the potential antimicrobial properties of olive extracts, we assessed their antibacterial and antifungal activities against a range of pathogenic microorganisms. This study included three Gram-negative bacteria (*E. coli*, *Y. pseudotuberculosis*, and *P. aeruginosa*), three Gram-positive bacteria (*S. aureus*, *E. faecalis*, and *B. subtilis*), and one yeast-like fungus (*C. albicans*). The effects of the extracts on these microorganisms, along with their MIC values, are presented in Table S9. While some extracts exhibited antimicrobial activity, others did not (Fig. S3). Specifically, none of the olive fruit or leaf extracts demonstrated activity against *B. subtilis*, *E. faecalis*, *P. aeruginosa*, *Y. pseudotuberculosis*, *E. coli*, or *C. albicans*, and their MIC values could not be determined. However, antimicrobial activity against *S. aureus* was observed in all fruit and leaf extracts except MF. The MIC values for *S. aureus* were recorded as 13.73 mg/mL for ML, 12.5 mg/mL for TL, 20 mg/mL for TF, 12.5 mg/mL for DL, and 30 mg/mL for DF extract. These findings suggest that while olive extracts exhibit selective antimicrobial properties, their activity is primarily restricted to *S. aureus*, with no detectable effects on other tested bacteria and fungi. Moreover, the antimicrobial activity of olive leaf extracts was higher than that of olive fruit extracts, and the highest MIC value was observed in the DF extract, indicating that the fruit extracts from Deştin had the weakest antimicrobial activity, emphasizing the trend of lower antimicrobial effectiveness in samples from the site farthest from the TPP.

Discussion

Proximity to the TPP decreases leaf and fruit biomass and essential mineral concentrations while increasing toxic element accumulation

Our findings indicate that proximity to the Yatağan TPP negatively impacts olive tree morphology and physiology, likely due to heavy metal-induced stress. Leaves and fruits from Şahinler (closest site) had significantly lower dry weights than those from Deştin (farthest site) (Fig. S1A-E, Table S3). This aligns with previous studies showing that plants near TPPs accumulate heavy metals like Cd, Pb, and Cr, which disrupt growth and mineral nutrient uptake³³.

While the accumulation of heavy metals and mineral imbalances are the primary factors affecting plant health in polluted environments, year-specific climatic conditions can also influence biomass production and mineral nutrient uptake. To assess this possibility, we compared the 2022 temperature and precipitation data with the 20-year averages (2004–2024) for Yatağan. The results indicated that the 2022 growing season was climatically typical, with only a 1.1% increase in average annual temperature and a 1.2% decrease in total precipitation compared to long-term means. In October, a critical month for fruit maturation, the temperature rose modestly by 2.5% and rainfall decreased by 2.2%. These slight deviations are unlikely to account for the substantial physiological and biochemical changes observed, suggesting that the proximity to the TPP and its

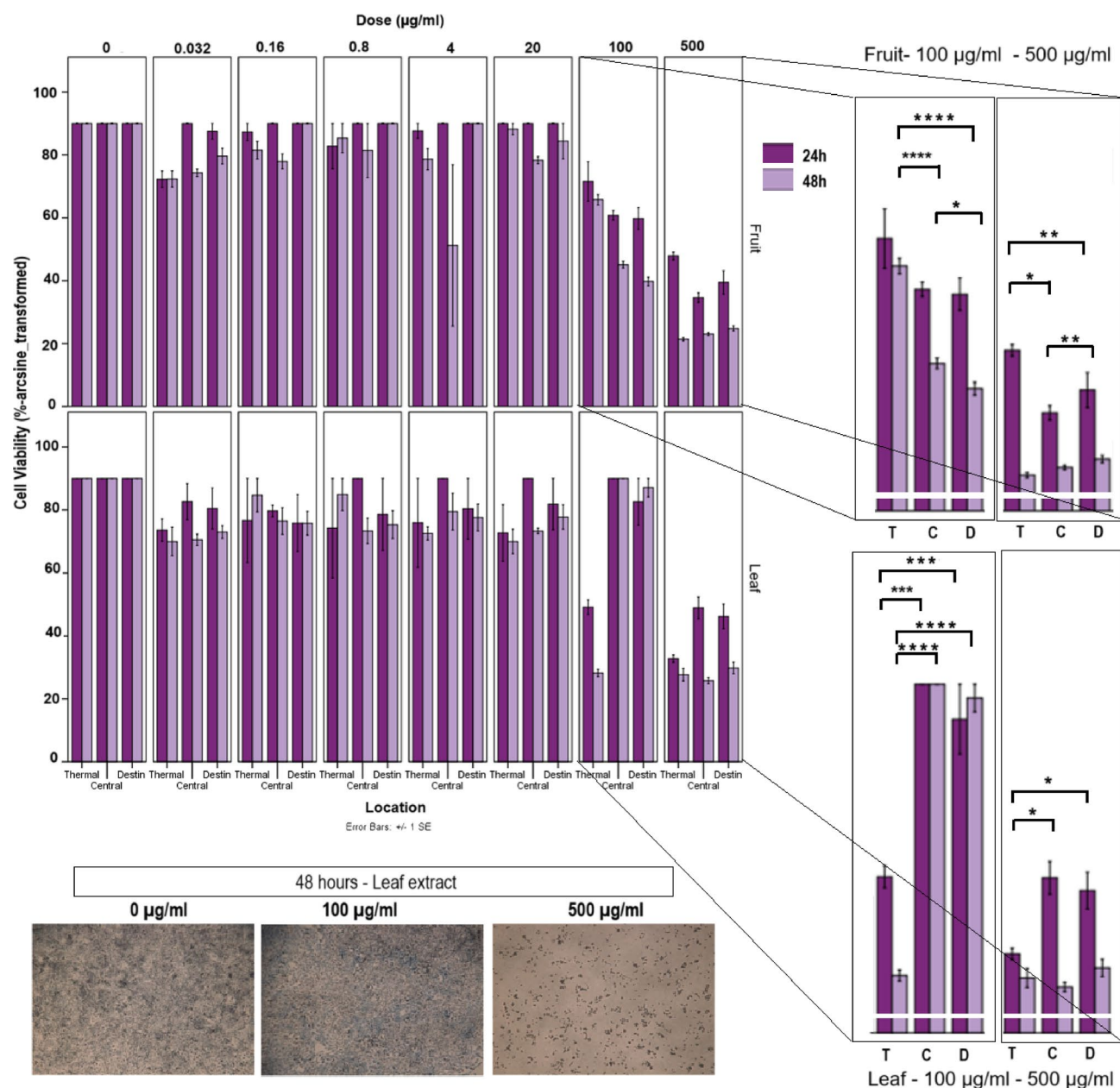


Fig. 6. The cell viability of BEAS-2B human bronchial epithelial cells treated with fruit (up panel) and leaf (down panel) extracts at varying concentrations for 24 h and 48 h. Extracts were obtained from olives grown at different distances from the Yatağan TPP, Deştin Village (farthest location), Central (middle location), and Thermal (Şahinler Village - closest location). Representative cells after the MTT assay are given after leaf extracts for 48 h (images taken by 5x objective of Zeiss AxioVert inverted microscope). Values represent mean \pm SEM ($n=3$). * $p < 0.05$, ** $p < 0.01$, *** $p < 0.001$, and **** $p < 0.0001$.

associated emissions remain the dominant factors driving the altered mineral nutrient profiles and growth patterns in olive trees.

Mineral nutrient uptake was notably disrupted near the TPP, with substantial reductions in key elements such as Ca, Mg, Fe, and Mn observed in Şahinler samples (Table 1). These deficiencies are likely related to soil acidification, cation competition, and the inhibitory effects of toxic metals such as Pb and Ni (Zaanouni et al. 2018). In contrast, elevated K concentrations may reflect shifts in soil pH or enhanced atmospheric deposition in polluted environments (J. Li et al. 2024; K. Lou Liu et al. 2020). Decreases in Na and S levels, despite coal combustion being a potential source of sulfur, may be attributed to changes in soil chemistry due to acidic deposition. These patterns are consistent with previous findings from the same region (Haktanir et al. 2010) and with studies in other Mediterranean olive-growing areas impacted by industrial pollution (Şahan and Başoğlu 2009).

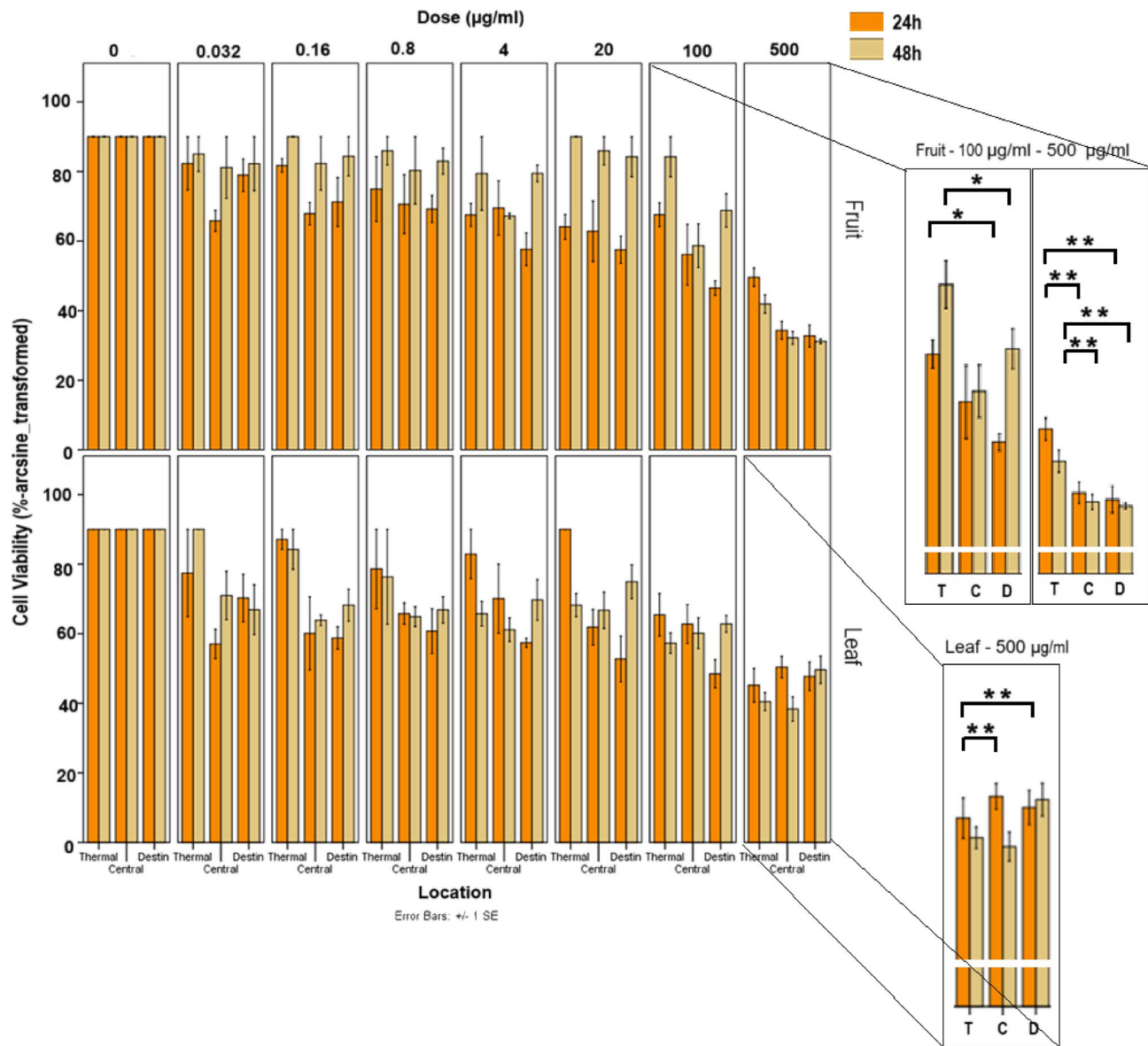


Fig. 7. The cell viability of HUVEC human umbilical vein endothelial cells treated with fruit (up panel) and leaf (down panel) extracts at varying concentrations for 24 h and 48 h. Extracts were obtained from olives grown at different distances from the Yatağan TPP, Deştin Village (farthest location), Central (middle location), and Thermal (Şahinler Village - closest location). Values represent mean \pm SEM ($n=3$). * $p<0.05$, ** $p<0.01$, *** $p<0.001$, and **** $p<0.0001$.

Differences in trace and potentially toxic element accumulation were particularly striking in samples from Şahinler, where markedly elevated levels of As, Cd, Cr, Hg, and Pb were observed in both leaves and fruits (Table 1). These findings suggest a strong influence of industrial emissions on elemental uptake and are consistent with previous studies reporting significant heavy metal accumulation in olive trees growing near thermal power plants, industrial sites, and high-traffic areas (Namuq 2022; Yücel and Kılıçoglu 2020; Petrella et al. 2018; Zaanouni et al. 2018; Şahan and Başoğlu 2009). A prior study analyzing olive leaves collected 4 km and 40 km from Yatağan TPP found that Cr, Ni, and Pb accumulated at toxic levels in the closer location, despite soil concentrations of these metals, except for Ni, remaining within normal ranges²⁶. Another study from the same region reported that sesame and carrot plants accumulated the highest Pb, Cu, Cd, and Zn concentrations depending on their proximity to the TPP²⁷. In that study, olive trees were also found to accumulate significantly higher levels of Pb and Cd, with concentrations exceeding permitted limits for edible vegetables. Although long-term irrigation with treated municipal wastewater has been shown to exacerbate metal uptake, causing Fe, Mn, Pb, and Zn to accumulate preferentially in olive roots, fruits, and leaves⁷ our results indicate that toxic metals such as As, Cd, Cr, Ni, and Pb accumulated significantly in olive leaves and fruits. Olive trees in other polluted regions, such as İzmir and Aydın, Türkiye, have exhibited similar contamination patterns, with Cd, Ni, and Cu transferring into fruits^{34,35}.

Heavy metal bioaccumulation poses significant health risks, especially for children, due to their toxicity and persistence in the food chain³⁶. High levels of metals like Pb and Cd pose health risks, making it crucial to monitor and control metal concentrations in olive oil^{37,38}. The significant elevation of toxic elements (As, Cd, Cr, Ni, Pb) alongside the reduction of essential nutrients (Ca, Mg, Fe, Mn) suggests that industrial emissions due to Yatağan TPP are altering soil and plant chemistry, leading to nutrient imbalances and potential toxicity. Similar patterns have been documented in studies from Tunisia and Türkiye, where heavy metal contamination from industrial activities has disrupted plant mineral nutrient uptake and raised concerns for human health through the food chain^{39,40}. The increase in toxic heavy metals interferes with the uptake and mobility of essential nutrients in olive trees. This supports the hypothesis that heavy metal contamination disrupts plant nutrition, leading to micronutrient deficiencies. Fe and Zn seem particularly affected, which is consistent with research showing that heavy metals like Pb and Cd inhibit Fe and Zn absorption in plants by competing with Fe/Zn for transporters (e.g., ZIP, NRAMP families)^{41–43} and bioavailability^{44,45} exacerbating essential micronutrient deficiency. While P and B remained stable, Mo levels were 125.6% higher in Şahinler leaves, indicating selective impacts of industrial pollution on different nutrients.

TPP has a negative effect on the nutritional value and quality of Olive leaves and fruits

Our analysis revealed that olive fruit extracts primarily contained major compounds such as oleuropein aglycone, nüzenide 11-methyl oleoside, and oleocanthal, while leaf extracts were rich in oleuropein, hydroxytyrosol, luteolin-7-glucoside, apigenin-7-glucoside, and verbascoside (Tables S4, and S5). These findings are consistent with Silva et al. (2010), who identified nüzenide and nüzenide 11-methyl oleoside as the main secoiridoids in olive seeds using LC-DAD-MS, and with Pereira et al. (2007)⁴⁶ (cited in¹, who reported oleuropein and these flavonoid glucosides as dominant phenolics in olive leaf extracts. Among the three sampling sites, Destin (farthest from the TPP) exhibited the highest diversity and concentration of these bioactive compounds, whereas Şahinler (closest to the TPP) had the lowest (Tables S4, and S5). These results indicate that proximity to the TPP negatively impacts the synthesis of secondary metabolites, aligning with reports that environmental pollution suppresses bioactive compound synthesis in medicinal plants⁴⁷. Since these compounds play crucial roles in plant defense and contribute to the nutritional and therapeutic value of olive products, this decline is significant. This metabolic shift in Şahinler samples may represent a trade-off strategy, where olive trees prioritize the synthesis of a narrower set of highly effective antioxidants over broader metabolic diversity. While this reprogramming likely enhances short-term survival under stress, it may compromise the overall nutritional and pharmacological value of the fruit by reducing the abundance of health-promoting secondary metabolites typically found in olives from cleaner environments. Such changes may also impact plant vigor, reproductive success, and long-term productivity in orchards near industrial pollution sources.

Heavy-metal exposure, particularly to Cd, Pb, Cu, and Ni, is known to disrupt redox homeostasis by inducing reactive oxygen species (ROS), which damage cellular macromolecules. To counteract this stress, plants activate enzymatic antioxidants (SOD, CAT, APX) and non-enzymatic secondary metabolites such as phenolics, flavonoids, proline, and phytochelatins^{48,49}. In olives, Cd stress promotes the accumulation of proline and antioxidant enzyme activity, which helps restore photosynthetic performance and growth⁵⁰. Similarly, phenolic biosynthesis is triggered in response to metal exposure. In a previous study, total phenolic content in olive leaves positively correlated with atmospheric Pb, Cu, and Mn loads near a Pb-contaminated oil refinery, supporting the idea that phenolic metabolism is activated as a defense strategy⁵¹.

Our findings are consistent with this stress-induced metabolic adaptation. While overall secondary metabolite content was lower in Şahinler samples, selective accumulation of specific flavonoids and phenolic acids, particularly apigenin and gallic acid, was evident. These compounds play vital roles in scavenging ROS, stabilizing membranes, regulating stress-response signaling, and mitigating cellular damage. Apigenin, a well-known antioxidant and anti-inflammatory compound⁵² was the dominant flavonoid in fruit extracts from Şahinler, while its glycosylated form, apigenin glycoside, was prevalent in the leaves, suggesting that the trees activated a targeted defense response through the accumulation of distinct flavonoid forms in different tissues (Tables S4, and S5). Apigenin scavenges free radicals and reduces oxidative stress, enhances mitochondrial function, induces apoptosis in cancer cells while sparing healthy cells by inhibiting angiogenesis and cell proliferation, promotes neuronal survival and protects against neurodegenerative diseases, and disrupts bacterial cell walls and membranes, making bacteria more susceptible to damage. Interestingly, apigenin and its derivatives accumulated only in Şahinler samples, suggesting that heavy metal-induced oxidative stress triggered their synthesis as a protective response. This accumulation could be an adaptive mechanism to counteract oxidative stress led by heavy metal accumulation, as apigenin is known for its protective roles against environmental stress⁵³. Similar stress-induced flavonoid accumulation, specifically apigenin, has been observed in chamomile flowers exposed to Cd toxicity⁵⁴. The selective accumulation in Şahinler samples may indicate that plants exposed to higher levels of heavy metals prioritize the production of specific flavonoids to enhance their resilience. In addition to apigenin and its derivatives, other secondary metabolites such as ferulic acid, luteolin, and luteolin glycoside were also detected in the leaves of trees close to the TPP. These flavonoids serve critical roles in plant metabolism, including protection against UV radiation, defense against pathogens, and regulation of metabolic processes⁵⁵.

Gallic acid (GA) was found high both in fruit and leaf extracts from the samples around TPP, and we have also detected a significant increase in Cd in both extracts. A study examined the effect of seed pre-soaking with GA on sunflower seedlings exposed to Cd stress suggesting that GA acts as a growth promoter under cadmium stress by strengthening the anti-oxidant defense system and protecting cellular integrity⁵⁶. Gallic acid treatment has made *Lepidium sativum* seedlings tolerant to salt stress⁵⁷. Significant accumulation of GA in the samples from Şahinler village suggests that olive plants may gain resistance to TPP-induced heavy-metal stress by GA's biological activity.

Besides, chlorogenic acid and caffeic acid, were only found in the leaf samples collected from Deştin, which is the farthest from the TPP. Oleocanthal phenolic compound was found in the fruit samples. Oleocanthal is a monophenolic secoiridoid, a group of antioxidants in some plant-based foods. Since this compound could not be detected in the fruits of olives grown in two regions near the TPP, it can be thought that the proximity of the olive plant to the TPP has a negative effect on nutritional value and quality. Since olive fruit is used directly as food, these negative effects may also have adverse effects on the human body. Oleocanthal has strong anti-inflammatory activities⁵⁸ and this was found only in the fruit extracts collected from the farthest location (Destin village). TPPs may prevent the production of oleocanthal and therefore can lower the nutritional yield of olive fruits. On the other hand, leaf extracts collected from around the TPP have ferulic acid. Ferulic acid was not a main content of leaves, however such apigenin-7-glycoside, vanillic acid, and caffeic acid were abundant in the leaves of *O. europaea*⁵⁹. Caffeic and chlorogenic acids were only found in the leaf extracts collected from Deştin village, while oleocanthal was the component only found in fruit extracts from Deştin village. Xie et al. found that one of the common contents of leaves and fruit is apigenin-7-β-D-glucose⁶⁰. Ünal et al. found that the concentrations of chromium, lead, zinc, and copper in the leaves of olive trees close to a factory in Izmir Kemalpaşa industrial zone (Türkiye) were higher than in the leaves of olive trees farther from the region⁶¹. The results of this study suggest that the closeness to the TPP affected the quantitative and qualitative features of leaves and fruits. Taken together, our findings showed that proximity to TPPs have negative impacts on olive plant metabolism due to heavy metal increase. These results raise critical questions about where and how TPPs should be established and demand immediate strategies to minimize their environmental and biological footprint. Future studies should investigate the molecular mechanisms behind these effects and explore ways to mitigate TPP-induced toxicity.

Leaf extracts of olives around TPP display the highest cytotoxicity in human cells

Cell culture studies showed that extracts of leaves collected from Şahinler village were more cytotoxic in human cells compared to the extracts of counterpart fruits. Leaves and fruits of *O. europaea* are reported to have anti-cancer effects on different cancer cell lines, and leaves also have an anti-hypertension and anti-microbial potential⁶². It was found that olive leaf extracts induced cytotoxicity in colon cancer cells, while these did not significantly affect normal human fibroblast cells⁶³. There are also many studies showed the cytotoxicity on breast cancer cells^{64,65} liver cancer cells (using commercial olive plants)⁶⁶ but not in normal cells such as human gingival and neutrophil cells⁶⁵ normal liver cells⁶⁶ and human mesenchymal stem cells⁶⁷. İşık et al. collected samples from three different suburbs of Balıkesir City; Ayvalık, Domat, and Uslu (Türkiye) which TPPs are not around these⁶⁷. Han et al. declared that they collected samples in Tunisia without any specific location⁶⁵. Many of these studies did not mention the location of the sample collection. These all suggest that olive plants are not harmful to normal human cells. However, there is no study to assess the effects of TPP on olive composition and their treatment.

A range of plants are contaminated with heavy metals from environmental factors. In this context, the detection of heavy metals in the extracts obtained especially from medicinal plants indicates that these plants may have a direct negative impact on human health. For instance, a high amount of copper was reported in the extracts of *Artemisia herba-alba*, a widely used medicinal plant for the digestive system and diabetes as well as against infection, collected from different locations in Jordan⁶⁸. Cadmium was found high in the extracts obtained from *Andrographis paniculata*, *Grona styracifolia*, *Houttuynia cordata* Thunb., and *Curcuma longa* L. purchased from different Chinese herbal markets in China⁶⁹. Lead (Pb) and cadmium (Cd) exposure significantly reduced human bone osteoblast viability in a concentration- and time-dependent manner, with cytotoxic effects observed at 0.1 μM after 48 h. Both heavy metals impair cellular bioenergetics, reducing ATP production, mitochondrial activity, and aerobic respiration while inducing oxidative stress through elevated reactive oxygen species (ROS), lipid peroxidation, and depletion of antioxidant defenses⁷⁰. In vivo studies also showed that heavy metals were associated with oxidative stress in many organs in the human body⁷¹. Thermal power plants are known to contaminate soils with heavy metals⁷². Maize cultivated near a coal-burning power plant in Bangladesh accumulated eight heavy metals (Ni, Cr, Cd, Mn, As, Cu, Zn, and Pb), with Zn and Cu being the most abundant in the soil⁷³. Olives grown around thermal power plants were also reported to accumulate heavy metals⁴⁰.

Ferulic acid was only found in the leaf extracts of olives collected around the TPP (Table S5). Ferulic acid is a biologically active compound in oxidative stress, inflammation, vascular endothelial injury, fibrosis, cell death, and even platelet aggregation⁷⁴. Apigenin was also another component increased in the samples from TPP. It has a function in the cell cycle arrest during different phases of proliferation, such as G1/S or G2/M by promoting several cyclin-dependent kinases and other genes⁷⁵⁻⁷⁷. This may result in cell death suggesting that it is therefore considered to have cytotoxic activity within the cells. However, olive is a well-known healthy food and is not supposed to be harmful to healthy human cells. Our study showed that environmental pollution by TPPs is associated with the cytotoxicity of olive leaves in healthy human cells.

Proximity to the TPP alters the antimicrobial activity of Olive fruits but not leaves

The in vitro antimicrobial and antioxidant activities of olive leaves and fruits against pathogenic bacteria and fungi have been demonstrated before⁷⁸⁻⁸². Studies have shown that olive leaf extracts effectively inhibit pathogens such as *Listeria monocytogenes*, *E. coli* O157:H7, *Salmonella enteritidis*⁸³ and *Candida* species⁸⁴. Similarly, olive leaves from Muğla province, Türkiye, demonstrated broad-spectrum antimicrobial properties, with the highest activity against *S. aureus*⁸⁵ similar to our findings. This suggests that olive genotype (Memecik cultivar) and environmental factors, including soil composition, climate, and irrigation, influence the production of antimicrobial phenolic compounds. Different olive cultivars exhibit variations in the concentration of phenolic compounds, such as oleuropein and hydroxytyrosol, which directly impact their ability to inhibit bacterial

growth⁸⁶. Moreover, soil fertility and nutrient availability can significantly alter the composition of phenolic compounds in olive leaves⁸⁷ while irrigation regimes alters the production of phenolics, such as oleuropein, in olive trees⁸⁸.

While TPP proximity did not affect the antimicrobial activity of leaf extracts, it significantly enhanced the activity of fruit extracts from Şahinler (the closest site) against *S. aureus* (Table S9). This may be due to increased phenolic compound accumulation or heavy metal exposure near the TPP. Similar findings were reported in olive trees near the Baniyas Oil Refinery, where Pb and Mn levels correlated with increased phenolic content. Furthermore, similar to our results, heavy metal exposure was shown to stimulate phenolic biosynthesis as a defense response to oxidative stress⁸⁹ which could explain the enhanced antimicrobial activity in fruits from the closest site to TPP. These results indicate the complex interplay between genetic and environmental factors in shaping the antimicrobial potential of olives. While olive leaf antimicrobial activity remains stable regardless of pollution exposure, TPP proximity appears to modulate fruit antimicrobial properties, potentially through stress-induced phenolic accumulation. Further research is needed to determine the precise mechanisms behind these changes and their implications for food safety and therapeutic applications.

Conclusion

This study provides the first comprehensive evaluation of how proximity to thermal power plants affects the biochemical composition of olive fruits and leaves, as well as the antimicrobial activity and cytotoxic effects of their extracts on healthy human cells. Our results indicate that industrial emissions disrupt mineral nutrient uptake in olive trees, markedly reducing essential elements like Ca, Mg, Fe, and Mn while increasing toxic metals such as As, Cd, Cr, Ni, and Pb. This elemental imbalance compromises the nutritional quality of olives and raises potential food safety concerns. In addition, our findings demonstrate that distance from the TPP plays a critical role in determining the secondary metabolite profiles of olive plants. Samples collected farther from the TPP exhibited a richer diversity and higher concentrations of key bioactive compounds. In contrast, plants closer to the TPP showed a selective accumulation of flavonoids, such as apigenin and its derivatives, which may represent an adaptive defense mechanism against heavy metal stress and pollutant exposure. Although this response helps counteract oxidative stress, it appears to come at the expense of reducing compounds that are nutritionally and pharmacologically important. Furthermore, olive leaf extracts from areas near the TPP exhibited significant cytotoxicity on human bronchial cells, suggesting that increased heavy metal accumulation may pose health risks. These observations highlight the importance of considering the distance from industrial sources when assessing the quality and safety of olive-derived products.

Critically, olive leaf extracts from areas near the TPP exhibited strong cytotoxicity, particularly on BEAS-2B bronchial cells, indicating potential human health risks associated with consumption or exposure. The alarming accumulation of heavy metals in olives, combined with their cytotoxic effects, highlights the urgent need for stringent environmental monitoring and regulation of industrial emissions. Without intervention, these disruptions to plant and soil chemistry could have cascading effects on agricultural sustainability, public health, and ecosystem stability.

Data availability

Data is provided within the manuscript or supplementary information files.

Received: 5 June 2025; Accepted: 29 August 2025

Published online: 21 October 2025

References

- El, S. N. & Karakaya, S. Olive tree (*Olea europaea*) leaves: Potential beneficial effects on human health. *Nutrition Reviews* vol. 67 632–638 at (2009). <https://doi.org/10.1111/j.1753-4887.2009.00248.x>
- Zhang, C. et al. Changes in phytochemical profiles and biological activity of Olive leaves treated by two drying methods. *Front Nutr* **9**, 854680 (2022).
- Elhrech, H. et al. Comprehensive review of *Olea europaea*: a holistic exploration into its botanical marvels, phytochemical riches, therapeutic potentials, and safety profile. *Biomol.* **2024**, 14, 722 (2024).
- Mbadra, C. et al. Heavy metals transfer in leaves, stem and roots of Olive tree near roads in the region of Sfax (Tunisia) and their impact on physiological characteristics. (2024). <https://doi.org/10.21203/RS.3.RS-3941162/V1>
- Cardoni, M. & Mercado-Blanco, J. Confronting stresses affecting Olive cultivation from the holobiont perspective. *Front. Plant. Sci.* **14**, 1261754 (2023).
- Mbadra, C. et al. Heavy metals transfer in leaves, stem and roots of Olive tree near roads in the region of Sfax (Tunisia) and their impact on physiological characteristics. *J. Essent. Oil Plant. Compos.* **3**, 76–94 (2025).
- Al-Hababeh, K. A. et al. Long-term irrigation with treated municipal wastewater from the wadi-musa region: soil heavy metal accumulation, uptake and partitioning in Olive trees. *Hortic.* **2021**, 7, 152 (2021).
- Wilson, B. & Pyatt, F. B. Heavy metal bioaccumulation by the important food plant, *Olea Europaea* L., in an ancient metalliferous polluted area of Cyprus. *Bull. Environ. Contam. Toxicol.* **78**, 390–394 (2007).
- Özkul, C. Heavy metal contamination in soils around the Tunçbilek thermal power plant (Kütahya, Turkey). *Environ Monit. Assess* **188**, 284 (2016).
- Turhan et al. Ecological assessment of heavy metals in soil around a coal-fired thermal power plant in Turkey. *Environ. Earth Sci.* **79**, 1–15 (2020).
- Mandal, A. & Sengupta, D. An assessment of soil contamination due to heavy metals around a coal-fired thermal power plant in India. *Environ. Geol.* **51**, 409–420 (2006).
- Cicek, A. & Koparal, A. S. Accumulation of sulfur and heavy metals in soil and tree leaves sampled from the surroundings of Tunçbilek thermal power plant. *Chemosphere* **57**, 1031–1036 (2004).
- Vig, N., Ravindra, K. & Mor, S. Heavy metal pollution assessment of groundwater and associated health risks around coal thermal power plant, punjab, India. *Int. J. Environ. Sci. Technol.* **20**, 6259–6274 (2023).

14. Pastrana-Corral, M. A. et al. Heavy metal pollution in the soil surrounding a thermal power plant in Playas de rosarito, Mexico. *Environ. Earth Sci.* **76**, 1–9 (2017).
15. Chen, Y. et al. A comprehensive review of toxicity of coal fly Ash and its leachate in the ecosystem. *Ecotoxicol. Environ. Saf.* **269**, 115905 (2024).
16. Petrović, M. & Fiket, Ž. Environmental damage caused by coal combustion residue disposal: A critical review of risk assessment methodologies. *Chemosphere* **299**, 134410 (2022).
17. Uğur, A., Özden, B., Saç, M. M. & Yener, G. Biomonitoring of 210Po and 210Pb using lichens and mosses around a uraniferous coal-fired power plant in Western Turkey. *Atmos. Environ.* **37**, 2237–2245 (2003).
18. Mentese, S., Yayintas, Ö. T., Bas, B., İrkin, L. C. & Yilmaz, S. Heavy metal and mineral composition of soil, atmospheric deposition, and mosses with regard to integrated pollution assessment approach. *Environ. Manage.* **67**, 833–851 (2021).
19. Le, L. T. et al. Environmental and health impacts of air pollution: A mini-review. *Vietnam J. Sci. Technol. Eng.* **66**, 120–128 (2024).
20. Altunoğlu, Y. & Yemişçioğlu, F. Determination of polycyclic aromatic hydrocarbons in olives exposed to three different industrial sources and in their respective oils. *Food Addit. Contam. Part. A.* **38**, 439–451 (2021).
21. Akgüpç, N., Özüyük, İ. İ., Yaşar, Ü., Leblebici, Z. & Yarıcı, C. Use of pyracantha coccinea roem. As a possible biomonitor for the selected heavy metals. *Int. J. Environ. Sci. Tech.* **7**, 427–434 (2010).
22. Tolunay, D. Dendroclimatological investigation of the effects of air pollution caused by Yatagan thermal power plant (Mugla-Turkey) on annual ring widths of Pinus brutia trees. *Fresenius Environ. Bull.* **12**, 1006–1014 (2003).
23. Cobanoglu, H., Sevik, H. & Koç, İ. Do annual rings really reveal cd, ni, and Zn pollution in the air related to traffic density?? An example of the Cedar tree. *Water Air Soil. Pollut.* **234**, 1–10 (2023).
24. Cesur, A. et al. The usability of Cupressus Arizonica annual rings in monitoring the changes in heavy metal concentration in air. *Environ. Sci. Pollut. Res.* **28**, 35642–35648 (2021).
25. Makineci, E. & Sevgi, O. Seyitömer Termik Santralinin Kuruma Alanlarindaki Karaçam (Pinus Nigra Arnold.) Yilik Halkalarina Etkisinin araştırılması. *Türkiye Orman Derg.* **6**, 11–22 (2009).
26. Yokaş, İ. et al. Research on pollution caused by thermal power plants in Muğla. *Int Meet Soil. Fertil. L Manag Agroclimatol Turkey* 997–1005 (2008).
27. Haktanır, K. et al. Muğla-Yatağan Termik Santrali Emisyonlarının Etkisinde Kalan Tarım ve Orman Topraklarının Kirlilik veri Tabanının oluşturulması ve Emisyonların Vejetasyona Etkilerinin araştırılması * generating pollution database of the agricultural and forest soils affe. *Ankara Üniversitesi Çevrebilimleri Derg.* **2**, 13–30 (2010).
28. Cecchi, L. et al. Virgin Olive oil by-product valorization: an insight into the phenolic composition of Olive seed extracts from three cultivars as sources of bioactive molecules. *Mol.* **2023**, 28, 2776 (2023).
29. Spagnuolo, C. et al. Phenolic extract from extra Virgin Olive oil induces different anti-proliferative pathways in human bladder cancer cell lines. *Nutrients* **15**, 1–20 (2023).
30. Demir, E. A., Colak, A., Uzuner, S. C. & Bekircan, O. Cytotoxic effect of a 3-(4-chlorophenyl)-5-(4-methoxybenzyl)-4H-1,2,4-triazole derivative compound in human melanoma cells. *Int. J. Biol. Chem.* **14**, 139–148 (2021).
31. Kumar, P., Nagarajan, A. & Uchil, P. D. Analysis of cell viability by the MTT assay. *Cold Spring Harb. Protoc. pdb.prot095505* (2018). (2018).
32. Kuete, V. et al. Antibacterial activities of the extracts, fractions and compounds from Dioscorea bulbifera. *BMC Complement. Altern. Med.* **12** 228, (2012).
33. Pathak, B., Rawat, K. & Fulekar, M. H. Heavy metal accumulation by plant species at fly-ash dumpsites: thermal power plant, gandhinagar, Gujarat. *Int. J. PLANT. Environ.* **5**, 111–116 (2019).
34. Turan, D. et al. The use of Olive tree (Olea Europaea L.) leaves as a bioindicator for environmental pollution in the Province of aydin, Turkey. *Environ. Sci. Pollut. Res.* **18**, 355–364 (2011).
35. Deliborlu, A. Environmental, ecological, and health risks assessment of Olive orchard soils in Izmir Province of Turkey. (2022). <https://doi.org/10.21203/RS.3.RS-1764874/V2>
36. Knezovic, Z., Trgo, M., Stipisic, A. & Sutlalic, D. Vukovar, Croatia,. Impact of metals from the environment on chemical changes in olive oil. in *International Scientific and Professional Conference 15th Ružička days* 103–112 (2014).
37. Rekik, O., Ben Mansour, A., Jabeur, H., Rodriguez Gutierrez, G. & Bouaziz, M. Effect of pollution on the quality of Olive oils from trees grown near a phosphoric acid factory. *Eur. J. Lipid Sci. Technol.* **121**, 1800490 (2019).
38. Liang, J. & Yang, W. Effects of zinc and copper stress on antioxidant system of Olive leaves. *IOP Conf. Ser. Earth Environ. Sci* **300**, 052058 (2019).
39. Zaanouni, N., Gharssallaoui, M., Eloussaief, M. & Gabsi, S. Heavy metals transfer in the Olive tree and assessment of food contamination risk. *Environ. Sci. Pollut. Res.* **25**, 18320–18331 (2018).
40. Şahan, Y. & Başoğlu, F. Heavy metal pollution in olives grown in bursa, Turkey. *Asian J. Chem.* **21**, 3023–3029 (2009).
41. Morina, F. & Küpper, H. Direct Inhibition of photosynthesis by cd dominates over Inhibition caused by micronutrient deficiency in the cd/Zn hyperaccumulator *Arabidopsis Halleri*. *Plant. Physiol. Biochem.* **155**, 252–261 (2020).
42. Bulut, H. Yıldırım doğan, N. Determination by molecular methods of genetic and epigenetic changes caused by heavy metals released from thermal power plants. *Appl. Biol. Chem.* **61**, 189–196 (2018).
43. Shen, Z., Chen, Y., Xu, D., Li, L. & Zhu, Y. Interactions between heavy metals and other mineral elements from soil to medicinal plant Fendgan (*Paeonia ostii*) in a copper mining area, China. *Environ. Sci. Pollut. Res.* **27**, 33743–33752 (2020).
44. Li, Y. et al. Effects of adsorption characteristics of different amendments on heavy metals (Pb, zn, and Cd). *J. Soils Sediments.* **20**, 2868–2876 (2020).
45. Yu, F., Ji, Y., Li, Z., Li, Y. & Meng, Y. Adsorption-desorption characteristics of typical heavy metal pollutants in submerged zone sediments: a case study of the Jialu section in zhengzhou, China. *Environ. Sci. Pollut. Res.* **30**, 96055–96074 (2023).
46. Pereira, A. P. et al. Phenolic compounds and antimicrobial activity of olive (*olea europaea* l. cv. *cobrançosa*) leaves. *Mol.* Vol. 12, Pages 1153–1162 12, 1153–1162 (2007). (2007).
47. Gurme, S. T., Ahire, M. L., Chavan, J. J. & Mundada, P. S. The influence of environmental pollution on secondary metabolite production in medicinal plants. *Environ. Pollut. Med. Plants.* 165–176. (2022). <https://doi.org/10.1201/9781003178866-9>
48. Handa, N. et al. Role of compatible solutes in enhancing antioxidative defense in plants exposed to metal toxicity. *Plants Under Met. Met. Stress Responses Toler Remediat.* 207–228. https://doi.org/10.1007/978-981-13-2242-6_7 (2018).
49. Goncharuk, E. A. & Zagorskina, N. V. Heavy metals, their phytotoxicity, and the role of phenolic antioxidants in plant stress responses with focus on cadmium: review. *Mol.* **2023**, 28, 3921 (2023).
50. Zouari, M. et al. Impact of proline application on cadmium accumulation, mineral nutrition and enzymatic antioxidant defense system of *Olea Europaea* L. cv Chelmlali exposed to cadmium stress. *Ecotoxicol. Environ. Saf.* **128**, 195–205 (2016).
51. Mahfoud, A. et al. An assessment study of usefulness of using Olive (*olea Europaea* l.) leaves in biomonitoring the air pollution near Baniyas oil refinery, syria: estimating of total phenolic compounds and lead, copper and manganese in Olive leaves. *Am. J. Plant. Sci.* **9**, 2514–2531 (2018).
52. Naponelli, V., Rocchetti, M. T., Mangieri, D. & Apigenin Molecular mechanisms and therapeutic potential against cancer spreading. *Int J. Mol. Sci.* **25**, 5569 (2024).
53. Gaur, K. & Siddique, Y. H. The role of apigenin in alleviating the impact of environmental pollutants. *Curr. Bioact. Compd.* **20**, E050324227673 (2024).
54. Zarinkamar, F., Moradi, A. & Davoodpour, M. Ecophysiological, anatomical, and apigenin changes due to uptake and accumulation of cadmium in matricaria Chamomilla L. flowers in hydroponics. *Environ. Sci. Pollut. Res.* **28**, 55154–55165 (2021).

55. Salehi, B. et al. The therapeutic potential of apigenin. *Int. J. Mol. Sci.* **20**, 1305 (2019).
56. Saidi, I., Guesmi, F., Kharbech, O., Hfaiedh, N. & Djebali, W. Gallic acid improves the antioxidant ability against cadmium toxicity: impact on leaf lipid composition of sunflower (*Helianthus annuus*) seedlings. *Ecotoxicol Environ. Saf* **210**, 111906 (2021).
57. Babaei, M., Shabani, L. & Hashemi-Shahraki, S. Improving the effects of salt stress by β -carotene and Gallic acid using increasing antioxidant activity and regulating ion uptake in *lepidium sativum* L. *Bot. Stud.* **63**, 1–10 (2022).
58. Pang, K. L. & Chin, K. Y. The biological activities of oleocanthal from a molecular perspective. *Nutr. 2018*. **10**, Page 570 (10), 570 (2018).
59. Benavente-García, O., Castillo, J., Lorente, J. & Ortúñoz, A. Del rio, J. A. Antioxidant activity of phenolics extracted from *Olea Europaea* L. leaves. *Food Chem.* **68**, 457–462 (2000).
60. Xie, P. et al. Phenolic compositions, and antioxidant performance of Olive leaf and fruit (*Olea Europaea* L.) extracts and their structure-activity relationships. *J. Funct. Foods.* **16**, 460–471 (2015).
61. Ünal, D., Sert, S., İşık, N. O. & Kaya, Ü. İzmir-Kemalpaşa Sanayi Bölgesinde Ağır metal Kirliliğinin biyoindikatör Olarak Zeytin (*Olea europaea*) Bitkisi Kullanılarak belirlenmesi. *Zeytin Bilim.* **2**, 59–64 (2011).
62. Alesci, A., Miller, A., Tardugno, R. & Pergolizzi, S. Chemical analysis, biological and therapeutic activities of *Olea europaea* L. extracts. *Natural Product Research* vol. 36 2932–2945 at (2022). <https://doi.org/10.1080/14786419.2021.1922404>
63. ÖzTÜRK, E., ÇALIK, F. & ULUSOY, D. Investigation of cytotoxic and genotoxic effects of Olive leaf extract on colon cancer cells and normal cell lines. *Eurasian J. Mol. Biochem. Sci.* **1**, 26–31 (2022).
64. Junkins, K., Rodgers, M. & Phelan, S. A. Oleuropein induces cytotoxicity and Peroxiredoxin over-expression in mcf-7 human breast cancer cells. *Anticancer Res.* **43**, 4333–4339 (2023).
65. Han, J., Talorete, T. P. N., Yamada, P. & Isoda, H. Anti-proliferative and apoptotic effects of Oleuropein and Hydroxytyrosol on human breast cancer MCF-7 cells. *Cytotechnology* **59**, 45–53 (2009).
66. Bektay, M. Y., Güler, E. M., Gökçe, M. & Kızıltas, M. V. Investigation of the genotoxic, cytotoxic, apoptotic, and oxidant effects of Olive leaf extracts on liver cancer cell lines. *Turkish J. Pharm. Sci.* **18**, 781–789 (2021).
67. İşık, S., Karagöz, A., Karaman, S. & Nergiz, C. Proliferative and apoptotic effects of Olive extracts on cell lines and healthy human cells. *Food Chem.* **134**, 29–36 (2012).
68. Abu-Darwish, M. S., Mohammad, M. Y., Abu-Darwish, D., Efferth, T. & Abu-Dieyeh, Z. H. Heavy metal contents in water extracts of selected medicinal plants used in the folk medicine of Jordan. *Phytomedicine Plus*. **4**, 100634 (2024).
69. Luo, L. et al. Heavy metal contaminations in herbal medicines: determination, comprehensive risk assessments, and solutions. *Front. Pharmacol.* **11**, 595335 (2021).
70. Al-Ghafari, A., Elmorsy, E., Fikry, E., Alrowaili, M. & Carter, W. G. The heavy metals lead and cadmium are cytotoxic to human bone osteoblasts via induction of redox stress. *PLoS One.* **14**, e0225341 (2019).
71. Mirkov, I. et al. Plant extracts and isolated compounds reduce parameters of oxidative stress induced by heavy metals: an up-to-date review on animal studies. *Curr. Pharm. Des.* **26**, 1799–1815 (2020).
72. Mandal, S., Bhattacharya, S. & Paul, S. Assessing the level of contamination of metals in surface soils at thermal power area: evidence from developing country (India). *Environ. Chem. Ecotoxicol.* **4**, 37–49 (2022).
73. Islam, M. S. et al. Toxicity assessment of heavy metals translocation in maize grown in the Ganges delta floodplain soils around the Payra power plant in Bangladesh. *Food Chem. Toxicol.* **193**, 115005 (2024).
74. Li, D. et al. Ferulic acid: A review of its pharmacology, pharmacokinetics and derivatives. *Life Sci.* **284**, 119921 (2021).
75. Iizumi, Y. et al. The flavonoid apigenin downregulates cdk1 by directly targeting ribosomal protein S9. *PLoS One.* **8**, e73219 (2013).
76. Maggioni, D. et al. Apigenin impairs oral squamous cell carcinoma growth in vitro inducing cell cycle arrest and apoptosis. *Int. J. Oncol.* **43**, 1675–1682 (2013).
77. Takagaki, N. et al. Apigenin induces cell cycle arrest and p21/WAF1 expression in a p53-independent pathway. *Int. J. Oncol.* **26**, 185–189 (2005).
78. Juven, B. & Henis, Y. Studies on the antimicrobial activity of Olive phenolic compounds. *J. Appl. Bacteriol.* **33**, 721–732 (1970).
79. Malhadas, C., Malheiro, R., Pereira, J. A., Guedes de Pinho, P. & Baptista, P. Antimicrobial activity of endophytic fungi from Olive tree leaves. *World J. Microbiol. Biotechnol.* **33**, 46 (2017).
80. Markín, D., Duek, L. & Berdichevsky, I. In vitro antimicrobial activity of Olive leaves. *Mycoses* **46**, 132–136 (2003).
81. Šimat, V. et al. Antioxidant and antimicrobial activity of hydroethanolic leaf extracts from six mediterranean Olive cultivars. *Antioxidants (Basel Switzerland)* **11**(9), 1656, (2022).
82. Borjan, D., Leitgeb, M., Knez, Ž. & Hrnčič, M. K. Microbiological and antioxidant activity of phenolic compounds in Olive leaf extract. *Molecules* **25** (24), 5946 (2020).
83. Liu, Y., McKeever, L. C. & Malik, N. S. A. Assessment of the antimicrobial activity of Olive leaf extract against foodborne bacterial pathogens. *Front. Microbiol.* **8**, 113 (2017).
84. Kinkela Devčić, M. et al. Antimicrobial activity of Olive leaf extract to oral *Candida* isolates. *Microorg* **2024**, **12**, 1726 (2024).
85. Baysal, G. et al. Determination of theoretical calculations by DFT method and investigation of antioxidant, antimicrobial properties of Olive leaf extracts from different regions. *J. Food Sci. Technol.* **58**, 1909–1917 (2021).
86. Pereira, J. A. et al. Table olives from portugal: phenolic compounds, antioxidant potential, and antimicrobial activity. *J. Agric. Food Chem.* **54**, 8425–8431 (2006).
87. Zhang, Y. et al. Effect of geographical location and soil fertility on main phenolic compounds and fatty acids compositions of Virgin Olive oil from leccino cultivar in China. *Food Res. Int.* **157**, 111207 (2022).
88. Talhaoui, N., Taamalli, A., Gómez-Caravaca, A. M., Fernández-Gutiérrez, A. & Segura-Carretero, A. Phenolic compounds in Olive leaves: analytical determination, biotic and abiotic influence, and health benefits. *Food Res. Int.* **77**, 92–108 (2015).
89. Seneković, J., Jelen, Š. & Urbanek Krajnc, A. Copper sulfate elicitation effect on biomass production, phenolic compounds accumulation, and antioxidant activity of *Morus Nigra* L. stem node culture. *Plants (Basel Switzerland)* **14**(5), 766 (2025).
90. Sukhdev, D. S. R. & Sukhdev, S. S. Google colabatory. *Google Cloud Platf. Data Sci.* 11–34. https://doi.org/10.1007/978-1-4842-9688-2_2 (2023).

Acknowledgements

The authors thank Prof. Nurettin YAYLI and Mrs. Gözde BOZDAL (Karadeniz Technical University) for assisting with leaf/fruit extractions, topographical engineer Mrs. Zeliha BAYRAM (İstanbul Municipality) for assisting with the use of Google Maps for finding locations, Prof. Zülfü ATLI ŞEKEROĞLU (Ordu University), Assoc. Prof. Hatice SEVİM NALKIRAN (Recep Tayyip Erdogan University), Dr. Cihan INAN (Karadeniz Technical University) for providing batches of BEAS-2B (ATCC, CRL-3588TM), ARPE-19 (ATCC, CRL-2302TM), and MC-F10A (ATCC, CRL-10317TM) cells, respectively, Prof. Kadriye INAN BEKTAS (Karadeniz Technical University) for assisting anti-microbial experiments, Mr. Ali GÜRBÜZ for collecting fruit and leaves, and METU Central Laboratory for ICP-MS analyses. HUVEC cells were purchased from ATCC (CRL-1730TM).

Author contributions

EG; Conceptualization, Methodology, Validation, Funding acquisitionEA; Conceptualization, Methodology,

Formal analysis, Investigation, Resources, Writing - Original DraftAS; Methodology, ValidationFBT; Methodology, Validation, Writing - Original DraftE\$; Methodology, ValidationNNK; Methodology, ValidationST; MethodologyHM; Conceptualization, Methodology, Resources, Writing - Review & Editing, Funding acquisitionMFK; Methodology, ValidationEAT; Methodology, Validation. Formal analysis, Investigation, Resources, Writing - Original Draft, Writing - Review & EditingSCU; Conceptualization, Methodology, Validation, Formal analysis, Investigation, Resources, Writing - Original Draft, Supervision, Project administration, Funding acquisition.

Funding

This study was supported by a 2209-A grant from TUBITAK (Project ID: 1919B012306896) and by Karadeniz Technical University (Project IDs: FLÖ-2024-11149, FLÖ-2024-11176 and FHD-2024-16036).

Declarations

Competing interests

The authors declare no competing interests.

Additional information

Supplementary Information The online version contains supplementary material available at <https://doi.org/10.1038/s41598-025-18066-y>.

Correspondence and requests for materials should be addressed to S.C.U.

Reprints and permissions information is available at www.nature.com/reprints.

Publisher's note Springer Nature remains neutral with regard to jurisdictional claims in published maps and institutional affiliations.

Open Access This article is licensed under a Creative Commons Attribution-NonCommercial-NoDerivatives 4.0 International License, which permits any non-commercial use, sharing, distribution and reproduction in any medium or format, as long as you give appropriate credit to the original author(s) and the source, provide a link to the Creative Commons licence, and indicate if you modified the licensed material. You do not have permission under this licence to share adapted material derived from this article or parts of it. The images or other third party material in this article are included in the article's Creative Commons licence, unless indicated otherwise in a credit line to the material. If material is not included in the article's Creative Commons licence and your intended use is not permitted by statutory regulation or exceeds the permitted use, you will need to obtain permission directly from the copyright holder. To view a copy of this licence, visit <http://creativecommons.org/licenses/by-nc-nd/4.0/>.

© The Author(s) 2025